ELSEVIER

Journal of Non-Crystalline Solids 263&264 (2000) 318–341

JOURNAL OF NON-CRYSTALLINE SOLIDS

www.elsevier.com/locate/jnoncrysol

Section 3. Applications

Nd-doped phosphate glasses for high-energy/high-peak-power lasers

J.H. Campbell *, T.I. Suratwala

Lawrence Livermore National Laboratory, P.O. Box 808, Livermore, CA 94550, USA

Abstract

The composition and properties of neodymium-doped (Nd-doped) phosphate glasses used for simultaneous high-energy (10^3–10^6 J) and high-peak-power (10^{12}–10^{15} W) laser applications such as fusion energy research, are reviewed. The most common base glasses are meta-phosphates (O/P ~3) with the approximate composition: $60P_2O_5$–$10Al_2O_3$–$30M_2O$/MO; K/Ba or K/Mg are typical modifiers. The spectroscopy of Nd^{3+} in these glasses is well understood and laser properties can be accurately determined from measured spectroscopic properties. The major mechanisms for Nd^{3+} non-radiative relaxation are reviewed and empirical expressions are presented that predict these effects in phosphate glasses. Optical and thermal–mechanical properties have been measured on a number of laser glasses and can be correlated with composition. Sub-critical crack growth rates in stress regions I, II and III have been reported for the first time in phosphate laser glasses. The mechanism for Pt inclusion formation and dissolution has been studied leading to damage resistant (Pt-inclusion-free) laser glasses.

1. Introduction

This review covers recent advances in phosphate laser glasses used for simultaneous high-energy and high-peak-power laser applications such as the multi-kilojoule, multi-terrawatt lasers used for fusion energy research [1–6]. Two new laser systems with output energies of nearly 2 MJ and peak-powers in excess of 500 TW are currently under construction [1,2]; both lasers will use neodymium-doped (Nd-doped) phosphate glasses [7,8]. This paper deals only with Nd-doped phosphate glasses as they represent the most common and largest volume of laser glass produced today [8].

Unfortunately, space prohibits us from reviewing the many developments of phosphate laser glasses using other rare-earth dopants or those used for fiber optics and wave-guided structures; the reader is referred to recent reviews and articles by others in this field (see for example [9–18]). Similarly, in the past there have been several excellent reviews of earlier work on both phosphate and non-phosphate laser glasses (silicates, borates, fluorides, fluorophosphates, aluminates, germanates, chalcogenides and sulfates) [16,19–29] and as a consequence that material is not covered here.

The manuscript is organized in sections dealing with key properties of laser glasses; the main exception is the brief review in Section 2 of the compositional space that has been studied during the development of Nd:phosphate laser glasses. Where possible the results are presented in a format that should be useful to both glass researchers and laser engineers for estimating key performance

* Corresponding author. Tel.: +1-925 422 6497; fax: +1-925 423 0972.

E-mail address: campbell12@llnl.gov (J.H. Campbell).

0022-3093/00/$ - see front matter
PII: S0022-3093(99)00645-6

properties of laser glasses. In addition we attempt to show why the laser glasses in wide use on multi-kilojoule/multi-terrawatt lasers have evolved to a specific set of metaphosphate compositions.

2. Phosphate laser glass composition development

Fig. 1 is a ternary composition diagram for the P_2O_5–(Al_2O_3,RE_2O_3)–(MO, M_2O) system showing the range of laser glasses that have been studied as well as the specific compositions of several commercial laser glasses produced today. Note that most of the commercial glasses lie near the line representing the metaphosphate join and have the approximate molar composition $60P_2O_5$–$10Al_2O_3$–$30M_2O$/MO. Nd is added to this base composition at concentrations of about 0.2 mol% ($\sim 5 \times 10^{19}$ ions/cm^3) for laser rods and up to 2 mol% ($\sim 5 \times 10^{20}$ ions/cm^3) for disks and plates [8,30,31].

The compositions of the three most widely used commercial metaphosphate laser glasses, LG-750, LHG-8 and LG-770, have recently been reported for the first time [7]: LHG-8: (56–60)P_2O_5–(8–12)Al_2O_3–(13–17)K_2O–(10–15)BaO–(0–2)Nd_2O_3, LG-750: (55–60)P_2O_5–(8–12)Al_2O_3–(13–17)K_2O–(10–15)BaO–(0–2)Nd_2O_3 and LG-770: (58–62)P_2O_5–(6–10)Al_2O_3–(20–25)K_2O–(5–10)MgO–(0–2)Nd_2O_3. The compositions are reported as ranges to account for variability due to doping and melting methods and protect certain proprietary aspects of the compositions [7]. Nevertheless, as discussed later in this manuscript, the laser, optical and physical properties of these three glasses are quite similar (±10%) suggesting that over these minor ranges in composition (and modifiers) the laser glass properties are largely unchanged. The reasons these specific modifiers and compositions make good laser glasses is discussed in several of the later sections.

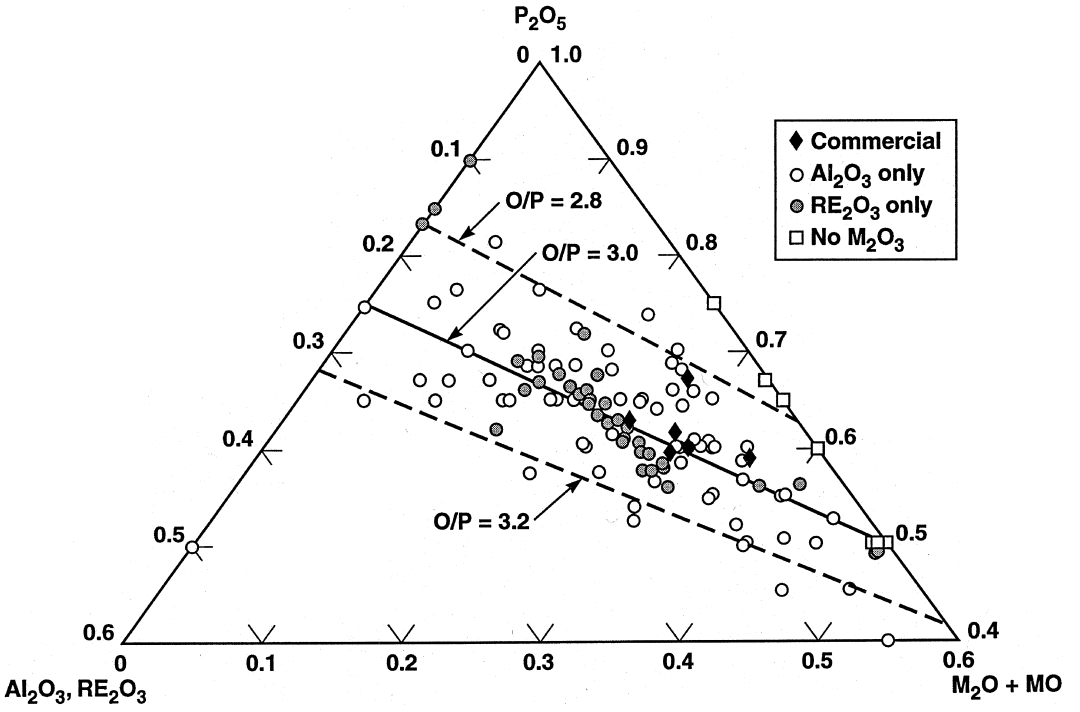

Fig. 1. P_2O_5–Al_2O_3,RE_2O_3–MO/M_2O composition diagram showing both research and commercial laser glass compositions. The sources for the research samples are given in Table 1; the compositions for the commercial glasses are from chemical analyses by the authors.

Table 1
Systematic composition studies of Nd phosphate laser glasses

Composition space	Fixed components	Varied components	Source
P_2O_5–Al_2O_3–M_xO	–	P, Al, Li, Na, K, Mg, Ca, Sr, Ba, Zn, Pb	[32]
P_2O_5–Al_2O_3–M_xO	Al	P, Na, Li, K, Cs, Mg, Ca, Ba	[34,35]
P_2O_5–Al_2O_3–M_2O–MO	Al	P, Na, Li, K, Ba	[36]
P_2O_5–Al_2O_3–M_2O–MO	–	P, Al, Li, Na, Ba, Ca	[37]
P_2O_5–B_2O_3–M_2O–MO	–	P, B, K, Na, Li, Ba, Sr, La	[38]
P_2O_5–Al_2O_3–SiO_2	–	P, Al, Si	[32]
P_2O_5–Nd_2O_3–SiO_2	–	P, Nd, Si	[32]
P_2O_5–SiO_2–Li_2O–Al_2O_3	–	P, Si, Li, Al	[32]
P_2O_5–Al_2O_3–M_2O–MO	P, Al	Li, K, Na, Mg, Ca, Ba	[39]
P_2O_5–Al_2O_3–Na_2O–MO	P, Al	Na, Mg, Ca, Ba	[40]
P_2O_5–Al_2O_3–Ln_2O_5–M_2O	–	Li, K, Nd, La, P, Al	[41]
P_2O_5–Al_2O_3–Na_2O–MO	P, Na	Al, Mg, Ca, Ba	[42]
P_2O_5–Al_2O_3–MO–M_2O	–	Be, Mg, Ca, Sr, Ba, Li, Na, K, Rb	[43]
P_2O_5–Al_2O_3–M_2O	P	Li, Na, K, Rb, Cs	[44]
P_2O_5–Al_2O_3–SiO_2–K_2O	P, K	Si, Al	[44]
P_2O_5–Al_2O_3–M_2O–MO	–	Al, Be, Mg, Ca, Sr, Ba, Cd, Li, Na, K, Rb	[20,23]
P_2O_5–SrO–K_2O	Sr	P, K	[45]
P_2O_5–K_2O–B_2O_3–MO	K, Ln	Sr, Ba, B, P	[45]
P_2O_5–K_2O–Ln_2O_3–Y_2O_3	K, Ln, Y	P	[45]

A number of systematic composition studies of phosphate laser glasses have been carried out. Unfortunately, these cannot all be represented in the single ternary diagram shown in Fig. 1. Instead we summarize many of these in Table 1. One of the most important systematic composition investigations is that reported by Toratani [32]. He examined not only laser properties but other key glass properties for the composition series P_2O_5–Al_2O_3–(M_2O, MO) with M = Li, Na, K, Mg, Ca, Sr, Ba, Zn and Pb. In addition, his compositions span the ultraphosphate to polyphosphate composition region. Also included in his work is an exploration of the P_2O_5–SiO_2–Al_2O_3, P_2O_5–SiO_2–Nd_2O_3 and P_2O_5–SiO_2–Al_2O_3–Li_2O glass forming systems. The latter system yielded a lithium silicophosphate glass with acceptable laser properties and much improved thermal shock resistance that was a forerunner of commercial glasses for high-average-power (HAP) applications [33].

Many composition studies [20,23,32,43–45], correlate variations in glass properties with modifier additions using the cation electric field-strength parameter [46]. Hayden et al. [39] extended this to include a compositionally averaged field strength that summed the contributions of the individual modifiers into one 'effective' field strength. They [39] were able to successfully correlate laser, optical, thermal and mechanical properties with the effective field strength parameter for a range of modifiers.

Although there is generally a variation in the M^+ or M^{2+} modifiers used in laser glasses, the M^{3+} modifier is nearly always Al^{3+}. Thus the role of Al^{3+} in metaphosphate laser glasses has been a subject of much interest. This interest is because Al^{3+} not only affects thermal–mechanical properties but also laser properties [20,32,47]. The most authoritative study of effects of Al^{3+} in phosphate glass structures is the work of Brow et al. [48–50]. They showed that physical property changes observed with addition of Al_2O_3 are predominantly due to cross-linking of the long metaphosphate chains by Al^{3+} in octahedrally coordinated sites ($Al(OP)_6$) [49,50]. This cross-linking is in contrast to the earlier-held view that the Al formed a three-dimensional network via the weaker tetrahedral $AlPO_4$ units. Also, Al^{3+} in the octahedral symmetry is the only form observed for $\leqslant 12.5$ mol% Al_2O_3 additive; at larger concentrations 4- and 5-fold coordinated Al are detected [50]. It is interesting that the optimum Al_2O_3 composition used in most commercial laser glasses is in the same $\leqslant 12.5$ mol% range (see Fig. 1).

Raman [32,51–54] and NMR [55–60] spectroscopy continue to be used to investigate phosphate

glass structures and many of these studies span the compositional region of interest for laser glasses (specifically, metaphosphate glasses). Unambiguous assignments have been made for many Raman bands such that these bands can now be used as a routine tool for structural investigations [54,61]. In one of the few Raman spectroscopy studies of just laser glasses, Toratani [32] and Izumatani et al. [62] reported spectra for each of the glasses in a systematic study of the P_2O_5–Al_2O_3–$MO(M_2O)$ composition space. Toratani used the data primarily to relate measured Nd^{3+} multi-phonon decay rates (from the $^4F_{3/2}$ level) to the most energetic phonon modes observed in a specific glass. Little structural interpretation has been given to his data although the Raman spectra show variations in band structure with changes in glass composition. Similarly, a number of glass structure studies using ^{31}P in combination with ^{27}Al, ^{29}Si, ^{11}B, ^{7}Li and ^{23}Na MAS NMR have been reported for phosphate glasses in general and metaphosphates in particular. Kirkpatrick and Brow have recently reviewed this work [60].

3. Laser properties derived from Nd spectroscopic measurements

The laser properties of Nd in a glass host are determined by the Nd^{3+} spectroscopic properties. In this section, we review recent research on Nd-spectroscopy in phosphate glasses and its relation to laser performance.

The electronic spectra of rare earths in crystalline and glass matrices has been the subject of investigation for more than 40 years. The excellent text by Powell [63] is perhaps the most recent authoritative account of the spectroscopy of transition metal and rare-earth lasant ions in crystalline and amorphous matrices; the reader is referred to this text and the references cited therein for further details.

The neutral Nd atom has the outer electronic configuration $4f^46s^2$ which, when incorporated in the glass gives Nd^{3+} with the ground electronic configuration $4f^3$. The energy levels associated with the $Nd^{3+}4f^3$ configuration are determined by the well-known, multi-electron atom Hamiltonian [63,64] (Fig. 2):

$$H = H_{\text{H-like}} + H_{\text{coul}} + H_{\text{SO}} + H_{\text{CF}} \tag{1}$$

$$= \left(\frac{-h^2}{2m} \sum_i^n \nabla_i^2 - Z_{\text{eff}} \sum_i^n \frac{e^2}{r_i} \right) + \sum_{i<j}^n \frac{e^2}{r_{ij}} + \lambda L \cdot S + \sum_i e V_{C_i}(r, \theta, \phi). \tag{2}$$

The terms inside the parentheses are sums of the individual (discrete) hydrogen-like kinetic and potential energy contributions summed over all n electrons of charge, e and mass, m. The electrons lie at distances, r_i, from the shielded nucleus that has an effective nuclear charge, eZ_{eff}. The next term, H_{coul}, accounts for the pair-wise electron coulombic repulsions where the restriction on i prevents double counting and r_{ij} is the pair-wise interelectronic separation. The third term, H_{SO}, describes the electron-spin and orbital-angular momentum interactions, where λ is the multi-electron spin–orbit coupling constant. Finally, the last term, H_{CF}, describes the electron perturbations, V_{C_i}, caused by the surrounding crystal field, where V_{C_i} is dependent on all three spatial coordinates (r, θ, ϕ). In general for Nd^{3+} in glass the magnitude of the various interactions described by the Hamiltonian in Eq. (1) are [63]

$$|H_{\text{H-like}}| \gg H_{\text{coul}} \gtrsim H_{\text{SO}} > H_{\text{CF}}. \tag{3}$$

The crystal field interaction (H_{CF}) is quite small because the rare earth 4f orbitals well shielded by the overlying $5s^2$ and $5p^6$ shells and therefore the states arising from the $4f^n$ configurations are only mildly affected by their surroundings [63,65]. The magnitude of the crystal field splitting for rare earths in glasses and crystals is of order 100 cm^{-1} (Fig. 2) and thus approximates kT at ambient temperatures (200 cm^{-1}). In addition, in most glasses, including phosphates, the Nd ions reside in sites of low symmetry (C_1) with each site having a slightly different crystal field interaction [63]. Therefore the Stark splittings associated with the crystal field perturbations cannot be individually resolved. This lack of resolution is represented in Fig. 2 by using broad, shaded bands to represent the site-to-site variation in the crystal field Stark splitting.

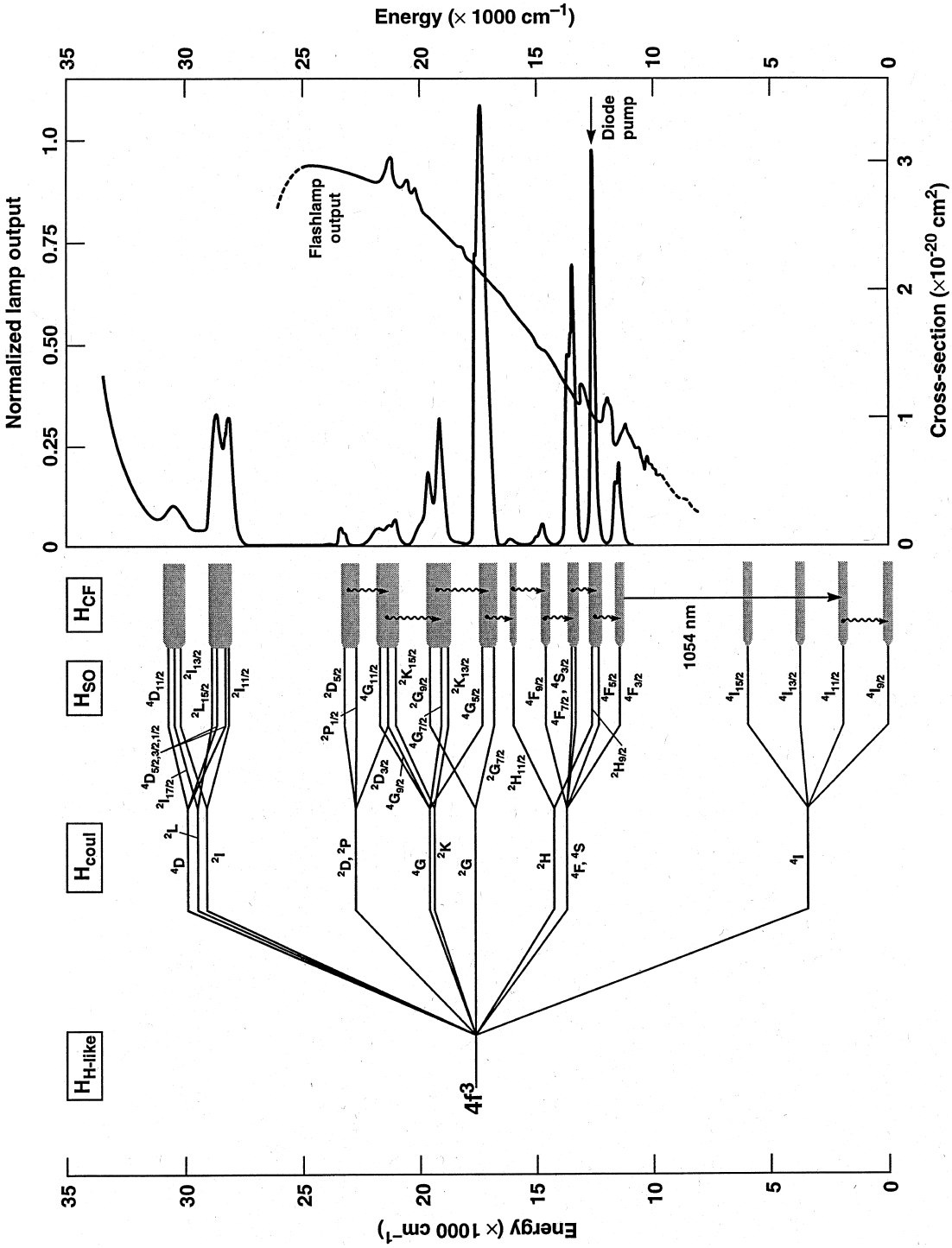

Fig. 2. Energy levels for Nd^{3+} evolving from the $4f^3$ configuration showing the coulombic (H_{coul}), spin–orbit coupling (H_{SO}) and crystal field (H_{CF}) interactions. Also shown is the measured Nd-absorption cross-section in a typical metaphosphate glass host [7] and the relative output intensity for a xenon flashlamp and laser diode pump source. The laser transition of interest (1053 nm) is from the metastable $^4F_{3/2}$ state to the $^4I_{11/2}$ terminal level. The wavy lines denote rapid non-radiative (multi-phonon) transitions. The energies shown are relative to the $^4I_{9/2}$ ground state.

The single-electron spin–orbit coupling constant is large for Nd, being a value of 884.6 cm^{-1} [64]. This large coupling constant is important for the laser performance of Nd^{3+} in that the J-state immediately above the ground state remains virtually unpopulated at ambient temperatures. The energy gap between the $^4F_{3/2}$ state and the terminal ^4I states, combined with the thermal isolation of the terminal laser levels from the ground state (see Fig. 2), gives Nd-doped materials their four-level lasing properties [66].

Fusion laser systems use the broadband output from a flashlamp to pump the large-aperture, Nd-doped glass laser amplifiers [67,68]. The typical spectral overlap of the output from a xenon flashlamp with the Nd^{3+} absorption (i.e. 'pump') bands is shown in Fig. 2 [30]. Beach et al. [69] have recently developed a unique diode-pumped glass rod amplifier for use in the smaller preamplifier systems of a fusion laser system. This amplifier uses a diode-bar array operating at 808 nm (12 400 cm^{-1}) and a unique lens duct to transport the diode output to the glass rod; the diode pumps the $^4I_{9/2}$ to $^4F_{5/2}$,$^2H_{9/2}$ transition (see Fig. 2). This diode pumped glass amplifier has been demonstrated using rods, 5 mm dia. × 50 mm long, of phosphate glass-doped with 4×10^{19} Nd ions/cm^3 [70].

The states above the $^4F_{3/2}$ level are split by energies of order 1000 cm^{-1} (Fig. 2). These energies are similar to the phonon energies of the glass matrix (~1100–1200 cm^{-1} for phosphates [32,71]) and therefore electrons excited to these levels relax by non-radiative multi-phonon processes. As a result, the electrons excited to these upper bands cascade down to the $^4F_{3/2}$ state where they become 'bottle-necked'. This bottle-neck is a result of the large energy gap (~5500 cm^{-1}) between the $^4F_{3/2}$ state and the lower-lying ^4I manifold (Fig. 2). The phonon coupling for this magnitude energy gap is poor and therefore radiative relaxation dominates [71]. Radiative transitions can occur to all the lower lying ^4I_J levels but the transition of greatest interest is the one to the $^4I_{11/2}$ level; this laser transition produces output radiation near 1053 nm in most phosphate glasses [23,30,66].

The electrons terminating in the $^4I_{11/2}$ state undergo non-radiative, multi-phonon decay to the ground state. This decay process must be fast compared to the pulse length of the laser for Nd^{3+} to operate as a four-level system. Bibeau et al. [72–74] have recently determined the decay rates from the $^4I_{11/2}$ to the $^4I_{9/2}$ ground state in several Nd-doped laser glasses using different measurement techniques. They report lifetimes between 250 and 450 ps for three commercial phosphate laser glasses (LG-750, APG-1 and APG-2). These decay times are such that they can affect laser performance for pulse-lengths less than 1 ns; Bibeau et al. [74] present a model that can be used to predict these performance effects. The megakilojoule lasers used for fusion energy research will operate at nominal pulse-lengths between 1 and 20 ns [1] and thus the performance should not be affected by the Nd^{3+} terminal level lifetime.

Payne and Bibeau [75] have extended this work to include measurements of the non-radiative decay rate from the $^4G_{7/2}$ to ($^4G_{5/2}$, $^2G_{7/2}$) state. These measurements were carried out on the same set of glasses (and some crystals) as used in the previous study [72]. The reason for studying this particular transition is that the energy gap is similar to that between the $^4I_{11/2}$ to $^4I_{9/2}$ levels. In addition, the decay rate is more amenable to direct measurement. The measured rate of decay from the $^4G_{7/2}$ state correlates to within about 15% with that measured for the $^4I_{11/2}$ state.

Payne and Bibeau [75] analyze their data using the Förster [76] and Dexter [77] theory for dipole–dipole energy transfer, treating the Nd ions as donors and the phonons as energy acceptors. From this theory they independently derive a form of the well-known energy gap law in which they separate the information regarding the host and rare earth (Nd^{3+}) into the exponential and pre-exponential factors, respectively.

To predict the performance of a laser amplifier containing a given Nd-doped glass medium requires knowledge of the Nd^{3+} laser properties for the particular glass (e.g., emission cross-section, radiative lifetime, etc.). In a classic paper, Krupke [78] showed how these laser properties can be accurately estimated for a given glass from measured Nd^{3+} absorption and emission spectra. Krupke's method, based on the Judd–Ofelt (J–O) treatment [79,80] of spectral intensities for trivalent rare earth ions, provided glass chemists with a means of

assessing key laser properties using straightforward spectroscopic measurements on glass samples from small-scale test melts. As a result, a large number of glass composition studies followed (e.g. [23,25,27,28,32,39,81]) and continue today [35,45,82–84]. The number of phosphate glass compositions studied in this fashion probably exceeds a thousand; in our laboratory alone we have evaluated several hundred individual phosphate glasses.

In the J–O treatment, the line strength, S, of a transition between the initial (J) and terminal (J') states is given by

$$S(aJ : bJ') = \sum_{t=2,4,6} \Omega_t |\langle aJ|U^{(t)}|bJ'\rangle|^2, \tag{4}$$

where a and b denote S, L and other quantum numbers that completely specify the state. The individual matrix elements $|\langle aJ|U^{(t)}|bJ'\rangle$ between the various J-states of the Nd $4f^3$ configuration have been calculated and are tabulated in readily available sources [23,63,78]. The J–O intensity coefficients (Ω_2, Ω_4 and Ω_6) are phenomenological parameters determined by a least-squares fit to the integrated absorption band strengths measured in the 400–950 nm (25 000–10 500 cm^{-1}) region [23]. The bands that are usually included in this calculation are shown in Fig. 2.

Once the J–O parameters are determined, it is straightforward to calculate the all-important emission cross-section at the peak wavelength from the relationship

$$\sigma(\lambda_p) = \frac{8\pi^3 e^2}{27hc(2J+1)} \left(\frac{\lambda_p}{\Delta\lambda_{eff}}\right) \frac{(n^2+2)^2}{n} S(aJ : bJ'), \tag{5}$$

where n is the refractive index at λ_p, the peak fluorescence wave wavelength, $\Delta\lambda_{eff}$ the effective bandwidth and the other constants have their usual meaning. The effective linewidth is determined from the measured fluorescence intensity ($I_f(\lambda)$) for the associated fluorescence transition

$$\Delta\lambda_{eff} = \int_{band} \frac{I_f(\lambda)\, d\lambda}{I_f(\lambda_p)}. \tag{6}$$

The cross-section determined by the J–O treatment is accurate to within ±10% provided the Nd-doping density has been accurately measured ($\leqslant \pm 1\%$).

The J–O method can also be used to calculate the radiative decay rate, k_r and the branching ratio, $\beta_{J'}$. The radiative decay rate is the sum of the individual radiative decay rates from the $^4F_{3/2}$ state to the ^4I terminal J′ states (see Fig. 2) and the branching ratio is the fraction of radiative transitions that terminate at a particular J′ state. The branching ratio depends on the ratio of the J–O intensity parameters, Ω_4/Ω_6 [23,63,85]. In general, Ω_4/Ω_6 is near-unity for most commonly used phosphate laser glass compositions [20,23,32] and therefore the branching ratios for the various Nd^{3+} fluorescence transitions are nearly the same. To be more specific, in meta-phosphate laser glass compositions approximately 50% of transitions terminate at the $^4I_{11/2}$ state, 40% at the $^4I_{9/2}$ state and 10% at $^4I_{13/2}$; typically less than 0.5% radiate to the $^4I_{15/2}$ state [20,23,86].

The emission cross-section (at the peak-emission wavelength), σ_{em}, is related to the other key spectroscopic properties through the expression

$$\sigma_{em} = \beta k_r \lambda_p^4 / (8\pi c n^2 \Delta\lambda_{eff}), \tag{7}$$

where β is the branching ratio, k_r, the radiative decay rate and the other terms have been defined previously. Tabulations of cross-sections, branching ratios and radiative decay rates have been published for a number of Nd-doped phosphate glass compositions as well as many other non-phosphate glass compositions (see, for example Ref. [23]).

Caird et al. [87] have determined the radiative lifetime and cross-section by direct measurement of the quantum yield. The quantum yield (ε) is the ratio of the measured fluorescence lifetime (τ_{meas}) to the radiative lifetime (τ_r)

$$\varepsilon = \tau_{meas}/\tau_r, \tag{8}$$

and represents the fraction of ions in the metastable state that can potentially produce emitted photons. Payne et al. [47] have also used this method to measure quantum efficiency for other phosphate laser glasses. The results show that the radiative lifetime determined by the J–O treatment and from the quantum yield method agree to

within about ±10% for the phosphate glasses they have measured. This number is in agreement with Krupke's original assessment of the accuracy for the J–O method for glasses [78].

Based on the combination of composition studies and laser property measurements that have been carried out to date, it is now possible to generalize about which metaphosphate glass compositions make the best glasses for high-energy laser applications. Results from the work by Toratani [32] on the system $MO–M_2O–Al_2O_3–P_2O_5$ perhaps best illustrate which compositions give the best laser performance (Fig. 3).

It is generally desirable that the laser glass used in multi-kilojoule laser system has a large emission cross-section, long fluorescence lifetime and narrow emission bandwidth [8,20,30,66,88]. The data show that K_2O is perhaps the best modifier and the Al_2O_3 content should be minimized because of its adverse effect on the cross-section. Furthermore, the laser properties also tend toward an optimum in the meta-phosphate to slightly ultra-phosphate composition region (60–65 mol% P_2O_5). Indeed, commercial laser glasses generally have compositions (see Section 2) close to that inferred from Toratani's data (Fig. 3).

Note that some Al_2O_3 must be added to the glass to improve its physical properties but in general the tendency is to decrease Al_2O_3 to as small as possible. Similarly, using K_2O as the only modifier is not practical, so each manufacturer has added a group II modifier: BaO in the case of LHG-8 and MgO for LG-770. MgO was chosen because it gives a smaller non-linear index [39] which improves the laser glass performance at larger intensities (see Section 6.1). Similarly, BaO is used because it improves physical properties (over K_2O alone) with little degradation of laser properties [32,39]. The output energies and peak-powers obtained using either LHG-8 or LG-770 are essentially identical [8] and both glasses have been successfully melted on a large-scale [7]. Other commercial phosphate glasses are near-meta-phosphates (see Fig. 1) and are in the same composition region.

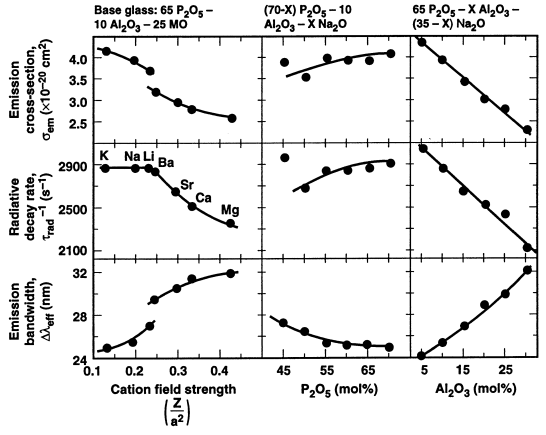

Fig. 3. Radiative decay rate, emission bandwidth and emission cross-section vs. compositional parameters derived from data reported by Toratani [32] for the ternary glass systems shown.

4. Non-radiative energy losses

Non-radiative energy losses from the $^4F_{3/2}$ state can reduce the stored energy and thereby affect the laser gain and overall system performance [20,63,66]. Non-radiative losses in phosphate laser glasses have been studied to such an extent that it is now possible to estimate the magnitude of most loss processes.

The rate of energy transfer, k_{total}, from the $^4F_{3/2}$ level is given by

$$k_{total} = k_r + k_{nr}, \tag{9}$$

where k_r is the radiative relaxation rate and k_{nr} the non-radiative rate. Experimentally the rate of energy transfer (k_{total}) is determined by measuring the fluorescence decay of the sample after it has been excited using a short-pulse pump source [23,47]. The measured decay rate can generally be fit using an exponential decay with characteristic time constant, τ_{meas}; thus in Eq. (9) $k_{total} = \tau_{meas}^{-1}$ and

$$k_{nr} = \left(\frac{1}{\tau_{meas}} - \frac{1}{\tau_r}\right), \tag{10}$$

where the radiative decay rate, k_r, is given by τ_r^{-1} and is independently determined using the J–O treatment (see Eq. (7)).

The non-radiative decay rate is a sum of contributions from all non-radiative processes [63]

$$k_{nr} = k_{mp} + k_{aug} + k_{Nd} + k_{OH} + \sum_{i=1}^{n} k_{TMi} + \sum_{j=1}^{m} k_{REj}. \quad (11)$$

The first three terms refer to loss by multi-phonon relaxation (k_{mp}), Nd self-quenching (k_{Nd}) and Auger up-conversion (k_{aug}). All three of these terms are intrinsic losses that depend on the glass structure and composition (Nd-doping level). The last three terms represent non-radiative losses due to impurities that enter during glass processing, specifically: hydroxyl groups (k_{OH}), transition metal ions (k_{TM}) and rare earth ions (k_{RE}) (e.g. [20,45,47,89,90]). Since there is the possibility of several transition metal or rare-earth impurities then the losses are given as a sum of the individual ion contributions [90]. Fig. 4 schematically illustrates each of the non-radiative loss processes.

Experimentally it is relatively straightforward to determine the contributions due to the last four terms in Eq. (11). This measurement is done by first preparing a 'reference' glass and then doping it with different concentrations of either Nd, OH or impurities (e.g. [89,90]). The increased decay rate due to the additive is then

$$k_{additive} = \tau_w^{-1} - \tau_{w/o}^{-1}, \quad (12)$$

where τ_w and $\tau_{w/o}$ are the measured fluorescence decay times with and without the additive, respectively.

4.1. Multi-phonon relaxation (k_{mp})

The rate of multi-phonon relaxation between two states can be described using an energy-gap law [20,71,72,75,91]

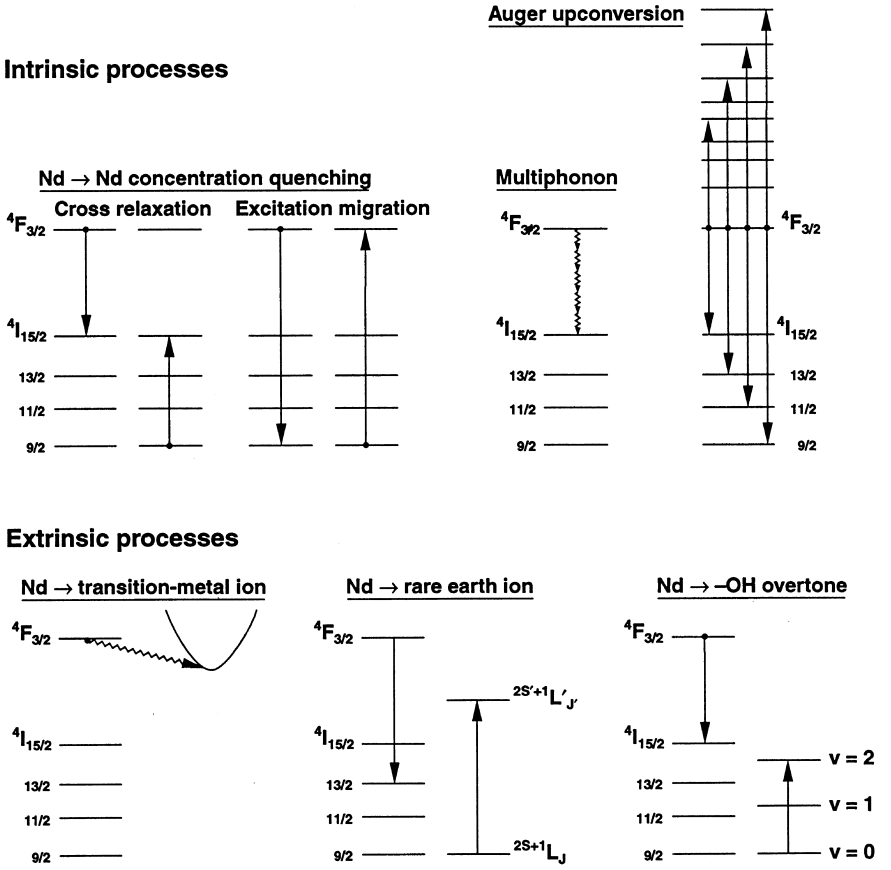

Fig. 4. Non-radiative Nd^{3+} relaxation processes in phosphate laser glasses.

$$k_{mp} = A\exp(-\alpha\Delta E), \tag{13}$$

where ΔE is the energy difference between the two states (cm^{-1}) and A and α are empirically derived constants. Layne et al. [71] report A and α of 4×10^{12} Hz and 4.61×10^{-3} cm, respectively, for a $67P_2O_5$–$15Na_2O$–18BaO phosphate glass. The measurements were made for excited states that were separated by about 2500–3900 cm^{-1}. Recently Bibeau et al. [75] have measured multi-phonon decay rates from the $^4G_{7/2}$ and $^4I_{11/2}$ states and report that these data also follow an energy gap law.

Direct measurement of the rate of multi-phonon decay from the $^4F_{3/2}$–$I_{15/2}$ state is difficult because the rate is less than a few hundred Hz. From extrapolation of the data from Layne et al. [71] and Bibeau et al. [75] to an energy gap of 5500 cm^{-1} ($^4F_{3/2}$–$^4I_{15/2}$) we get a rate of only about 150 Hz. Measurements by Caird et al. [87] on two commercial phosphate glasses (LG-750 and LG-760) are consistent with this observation; the measured multi-phonon relaxation rate is about 220 ± 120 Hz. The data from the above-mentioned studies are shown in Fig. 5; a least-squares fit of Eq. (13) to the data gives A and α of 2.4×10^{12} Hz and 4.35×10^{-3} cm, respectively. These numbers are in agreement with those originally reported by Layne et al. [71].

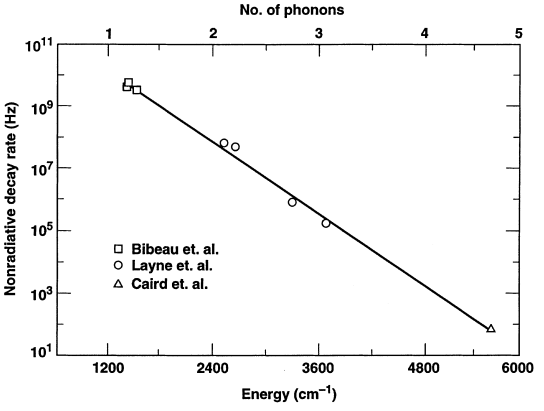

Fig. 5. Rate of Nd^{3+} multi-phonon relaxation in phosphate glasses vs. energy gap between J-states, based on data from Bibeau et al. [73], Layne et al. [71] and Caird et al. [87].

4.2. Nd-concentration quenching (k_{Nd})

The study of Nd self-quenching in laser glasses has received perhaps the most attention of all the non-radiative decay processes. One reason for such scrutiny is that most multi-kilojoule lasers use glass disks or slabs with Nd-doping densities which maximize the pumping efficiency (pump light absorption) and the stored energy density [30]. Concentration quenching refers to the energy exchange between a pair of Nd ions and is the result of two relaxation mechanisms (Fig. 4) [63]. One is cross-relaxation in which two neighboring ions exchange energy and the second is migration of the excitation energy from one ion to the next (the so-called 'hopping' mechanism). In theory the rate of relaxation due to concentration quenching varies as r^{-6}, where r is the inter-ion distance; note that the r^{-6} dependence is physically equivalent to the square of the Nd^{3+} concentration. In reality the effect of the Nd concentration on relaxation rate is dependent on the glass composition and varies from near-linear in ultra-phosphates to quadratic in near-metaphosphates and from quadratic to cubic in silicates [20,41,45,47,86,87,92,93].

The empirical relationship commonly used to describe concentration quenching in metaphosphate laser glasses is [47]

$$k_{Nd} = k_0(N/Q)^2, \tag{14}$$

where k_0 is the zero concentration decay rate, k_{Nd} the increased decay rate due to the presence of Nd (see Eq. (11)), N the Nd^{3+} ion concentration (cm^{-3}) and Q (cm^{-3}) is an empirically determined quantity for a given glass. Q is physically equivalent to the Nd concentration needed to reduce the lifetime to one-half its zero concentration limit (i.e., twice the zero-concentration decay rate). The parameter, Q, has been reported to vary linearly with the emission bandwidth for a number of phosphate laser glasses (Fig. 6) [47]. This trend is physically reasonable on the basis of the Förster/Dexter theory [76,77] for dipolar energy transfer because the rate of concentration quenching is related to the extent of spectral overlap between the two adjacent Nd ions. Therefore greater

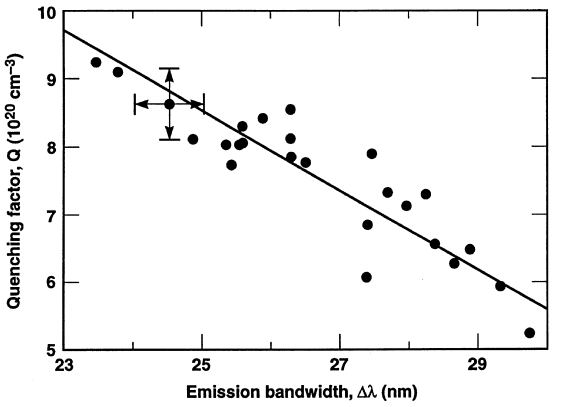

Fig. 6. Measured Nd concentration quenching factor (Q) vs. the measured emission bandwidth for a series of multi-component metaphosphate laser glasses, based on data from [47].

concentration quenching rates are expected for glasses with greater emission bandwidths.

Fig. 7 shows the concentration quenching rate measured for samples of two commercially available meta-phosphate laser glasses commonly used in high-energy applications: LHG-8 and LG-770 [8]. Both have a linear dependence of decay rate with the square of the Nd-doping concentration as predicted by Eq. (14); measurement errors are within the size of the data symbols.

Caird et al. [87] have reported Nd concentration quenching effects in LG-750 and LG-760. They have measured the quantum efficiency over a concentration range from about 0.2 to 13×10^{20} Nd^{3+}/cm^3 and analyzed the non-radiative decay using the Förster [76] model for cross-relaxation, but modified for energy migration using Burshtein's [95] 'hopping' model. The results show that both mechanisms are needed to model the change in quantum efficiency with Nd concentration; however, cross-relaxation appears to be the dominant relaxation mechanism in these glasses.

Lunter et al. [81] report the affects of Group I modifier ions on the rate of concentration quenching in an ultraphosphate laser glass and show that the quenching increases from Cs to Li. They also show that the quenching rate increases linearly rather than quadratically with Nd-concentration in agreement with the work of Stokowski on ultraphosphates [20]. The relaxation rate can be represented by the expression

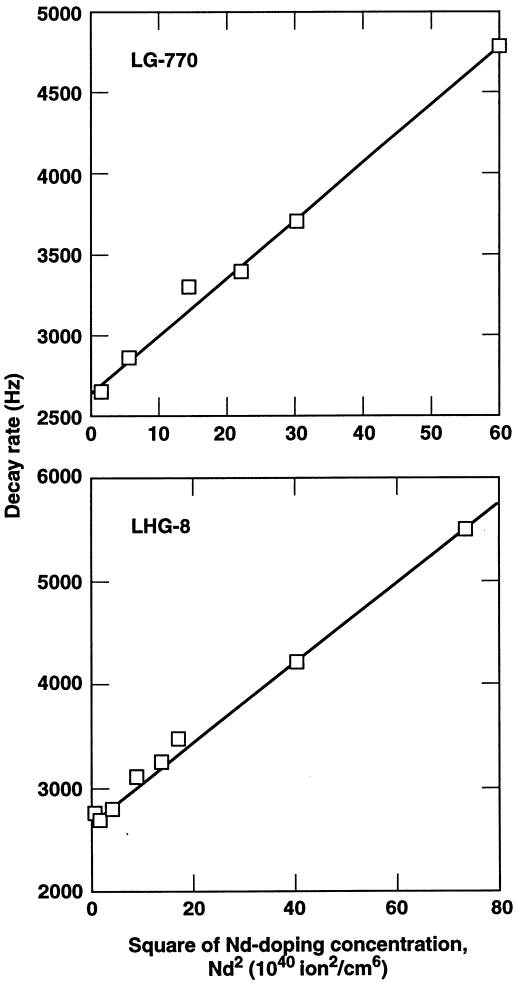

Fig. 7. Nd concentration quenching in LHG-8 and LG-770 metaphosphate laser glasses based on data reported in [8,94]; the measurement errors are within the symbol size.

$$(k_{\text{meas}} - k_0) = A[\text{Nd}], \tag{15}$$

where k_{meas} is the measured transition rate, k_0 the rate in the absence of concentration quenching and A is a constant for any given cation. Fig. 8 shows that the quantity A, determined from the slope of the decay rate data reported by Lunter et al. [81], increases with the cation field strength (Z/a^2).

Jiang et al. [96] report measurements of Nd^{3+} concentration quenching in the two glasses

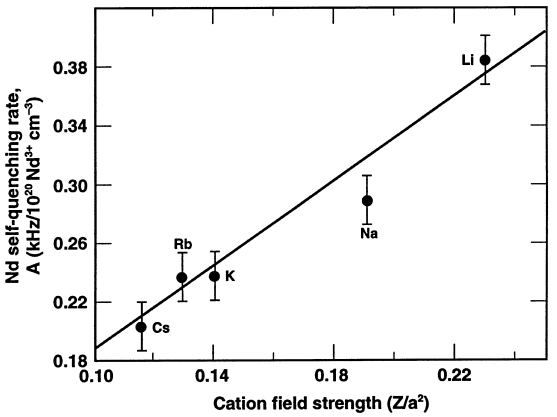

Fig. 8. Correlation of Nd self-quenching rate with modifier electric field strength; generated from data reported by Lunter et al. [81].

$18K_2O$–$10Al_2O_3$–$6Ln_2O_3$–$66P_2O_5$ and $26Li_2O$–$10Ln_2O_3$–$64P_2O_5$. The glass containing the Li modifier had a much greater quenching rate. This trend agrees qualitatively with the results from Lunter et al. [81], although the effect of the small amount of Al_2O_3 used in one of the Jiang et al. glasses raises some uncertainty.

The effect of a systematic change in the group II modifiers on Nd concentration quenching is reported in the work by Byun et al. [97]. They use a Nd^{3+}-doping range of $0.2–10 \times 10^{20}$ ions/cm^3 in two meta-phosphate glasses: $45RO–2.5Al_2O_3–52.5P_2O_5$ and $35RO–10Na_2O–2.5Al_2O_3–52.5P_2O_5$ (R = Mg, Ca or Ba). The data show a trend Ba < Ca < Mg in increased Nd self-quenching. This trend agrees with the trend observed for the group I oxides (Fig. 8) in that the quenching rate increases with modifier field strength.

Ebendorff-Heidepriem et al. [45] report Nd concentration quenching measurements in the two meta-phosphate glasses $Sr(PO_3)_2$ and $11K_2O–28BaO–6Al_2O_3–55P_2O_5$ doped with between about 1 and 10×10^{20} Nd^{3+}/cm^3. The decay rates vary linearly with the square of the Nd concentration as predicted via a dipolar relaxation mechanism (see Eq. (14)) similar to that reported above for other metaphosphates. In agreement with the work discussed above, Ebendorff-Heidepriem et al. [45] also conclude that using low field strength modifiers, such as K and Ba, reduces the concentration quenching. They suggest that the large difference in field strength between K^+ (and Ba^{2+}) and Nd^{3+} produces a regular alteration in positions of the two cation polyhedra (Nd and K) along the meta-phosphate chains and thus maximizes the separation between Nd^{3+} ions. They propose that such an alteration would not occur for modifiers having field strengths comparable to Nd^{3+} (e.g., Y^{3+}).

The data from the above studies [40,45,81,96] show that laser glass compositions with the smallest concentration quenching effects are those glasses that use groups I and II cations with the smallest electric field strengths. The data indicate that K and Ba should give the best results and indeed one or both of these two modifiers are used in commercial laser glass compositions (see Section 2).

4.3. Auger up-conversion losses (k_{Aug})

Until recently, Auger up-conversion loss had not been reported in Nd-doped laser glasses. Auger up-conversion occurs when two excited Nd ions, both in the metastable $^4F_{3/2}$ state, interact such that one ion returns to a lower-lying ^4I_J state while the other is excited to an energetically equivalent higher state (see Fig. 4). Payne et al. [98] have recently measured up-conversion losses in two phosphate laser glasses (APG-2 and LG-770), a silicate (LG-660) and the heavy metal fluoride glass, ZBLAN. They report that the product of the emission lifetime (τ) and the Nd up-conversion constant (γ_A) (i.e., $\gamma_A\tau$) is nearly constant for these materials and between 1 and 2×10^{20} cm^3. The γ for LG-770 is 8.1×10^{-17} (cm^3/s) ±30% [98].

The kinetic equation describing the decay from the $^4F_{3/2}$ state depends on the Nd excited state concentration [98]. The contribution of the up-conversion process to increased Nd decay rate, k_{Aug}, can be approximated as

$$k_{Aug} \approx \gamma_A N^*, \tag{16}$$

where N^* is the excited state density. N^* is about 10^{18} cm^{-3} in glasses used in most high-energy laser applications (i.e., stored energy about 0.25 J/cm^3 [88]). Thus, the increased decay rate due to up-conversion loss (via Eq. (16)) is less than 100 Hz.

4.4. Hydroxyl group effects on non-radiative decay rate (k_{OH})

A number of researchers have reported either OH quenching rates or data from which it can be easily derived [20,32,94,96,99]. In several cases the measurements have been made as a function of Nd concentration in various phosphate glasses; Fig. 9 summarizes these data. The data are valid for –OH concentrations (as measured by the absorption at $\sim$3000 cm^{-1}) up to about 10 cm^{-1}.

A simple empirical relation that can be used for estimating the magnitude of OH quenching in Nd–phosphate glasses at a given Nd concentration is [47]

$$k_{OH} = Q_{OH}(\alpha_{OH}), \tag{17}$$

where α_{OH} is the absorption coefficient at 3000 cm^{-1} due to OH and Q_{OH} is the quenching coefficient (Hz/cm^{-1}) determined from Fig. 9. The OH quenching rate increases nearly linearly with Nd concentration at doping levels $\geqslant 3 \times 10^{20}$ ions/cm^3. However at doping levels $< 1 \times 10^{20}$ ions/cm^3 the quenching rate approaches a constant of about 60 Hz/cm^{-1}. The trend at low doping is unexpected. Based on a simple dipolar relaxation mechanism [22,63] for uniformly distributed donor (Nd) and acceptor (OH) centers one would expect the OH quenching rate to vary linearly with Nd concentrations at low dopings and to pass through the origin. The data in Fig. 9 are fit to an empirical expression $Q_{OH} = a + b[Nd]^{3/2}$, where a is 62.8 Hz cm and b is 7.26×10^{-30} Hz cm/(ions/cm^3)$^{3/2}$. This expression has no theoretical significance and simply represents a best-fit to the data over the range shown.

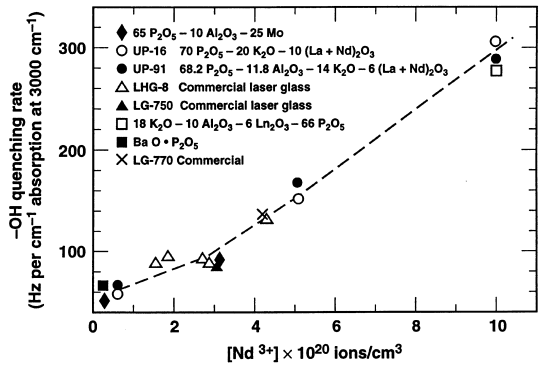

Fig. 9. Nd fluorescence quenching rate (Q_{OH}) due to –OH contamination for phosphate glasses with various Nd concentrations. The dashed line is fit to the data using an empirical expression discussed in the text. *Sources*: [20,32,47,94,96,99].

To achieve optimum laser performance, the hydroxyl group absorption should be less than 2.0 cm^{-1} at 3000 cm^{-1} [7,43]. An absorption of 2 cm^{-1} corresponds to about 200 ppmw of OH [7], however, absolute measurements of OH content in phosphate glasses are difficult, particularly at concentrations less than 1000 ppmw. Conversion factors for relating the absorption coefficient at $\sim$3000 cm^{-1} to absolute OH concentrations vary from about 30 to nearly 400 ppmw/cm^{-1} with most factors between about 60 and 130 ppmw/cm^{-1} [100]. This range of data has prompted Ebendorff-Heidepreim and Ehrt [101] to suggest that only absorption measurements should be used as a measure of the relative –OH content in glasses.

4.5. Fluorescence quenching by rare earth and transition metal ions

The absorption bands of some rare earth (RE) and transition metal (TM) ions overlap the Nd^{3+} 1053 nm emission band. This spectral overlap leads to fluorescence quenching as described by the Förster/Dexter theory [76,77] for dipolar energy transfer. Some RE and TM ions absorb enough at 1053 nm that they affect the Nd fluorescence decay rate at concentrations less than 10 ppmw [20,89,90]. Stokowski and Krashkevich [89] examined the effects of transition metal ions (Cu, Fe, V, Cr, Co and Ni) doped at 300 ppmw on Nd quenching in an ultraphosphate glass at different Nd-doping levels. Ehrmann et al. [90] report quenching rates for Cu and Fe at one Nd-doping concentration but for a range of impurity levels from about 30 to 1000 ppmw. The Cu quenching rate (reported in Hz/ppm impurity) is constant at all impurity concentrations. In contrast, the Fe quenching rate decreases at doping levels <300 ppmw; Ehrmann et al. [90] attribute this decrease to a change in the Fe^{2+}/Fe^{3+} ratio.

5. Absorption and scattering losses

The net gain of a glass laser amplifier is a function not only of the gain coefficient but also the combined passive transmission losses in the glass due to impurity absorption and scattering [66,90]. The total static absorption loss, α_{total}, in laser glass at 1053 nm is a sum of contributions

$$\alpha_{\text{total}} = \alpha_{\text{Nd}} + \sum_{i=1}^{n} \alpha_{\text{TM}_i} + \sum_{j=1}^{m} \alpha_{\text{RE}j} + \alpha_{\text{OH}}, \tag{18}$$

where the four terms on the right side refer to absorption losses due to: (1) Nd^{3+} ions thermally populating the terminal laser level ($^4I_{11/2}$), (2) transition metal ion impurities, (3) rare earth ion impurities and (4) residual hydroxyl groups, respectively. These impurities may originate from the glass raw materials, the melter refractory and/or impurities from an outside contamination source. Commercially supplied laser glasses typically have an un-pumped absorption loss of less than 0.0015 cm^{-1} at 1053 nm [31]. For ICF laser systems, the typical gain coefficient through a flashlamp pumped laser slab doped with 2–4×10^{20} Nd^{3+}/cm^3 is about 0.05 cm^{-1} [88]. Therefore, the ratio of gain-to-loss coefficients is greater than about 30:1. To achieve these gain-to-loss levels requires the use of raw materials as well as melter wall materials with the impurity concentrations typically less than 10–100 ppmw, depending on the TM or RE ion [7,90,102].

The Nd^{3+} absorption cross-section for the $^4I_{11/2}$ to $^4F_{3/2}$ transition at room temperature in a meta-phosphate glass is reported as [94]

$$\alpha_{\text{Nd}}(T) = 1.03 \times 10^{-20} \exp(-2576/T)[\text{Nd}^{3+}], \tag{19}$$

where $\alpha_{\text{Nd}}(T)$ is the temperature-dependent absorption coefficient (cm^{-1}) and $[Nd^{3+}]$ is the Nd ion concentration (ions/cm^3). Eq. (19) should provide reasonable estimates (±15%) for static Nd^{3+} absorption losses in other meta-phosphate glasses in the absence of direct measurements.

Ehrmann et al. [90] have compiled extinction coefficients at 1053 nm reported for phosphate laser glasses doped with various transition metal and rare earth ion impurities [89,90,102–104] and melted under oxidizing conditions (1 atm O_2). Currently most phosphate laser glasses are processed under oxidizing conditions so iron contamination tends to occur mainly as Fe^{3+} in meta-phosphate laser glasses [90,104,105]. Fe^{3+} absorbs in the visible and UV [106–109] and has insignificant absorption near the 1053 nm laser transition. Nevertheless, some equilibrium amount of Fe^{2+} is usually present which has an absorption band near 1000 nm [105,110–112]. The Fe^{2+}/Fe^{3+} distribution in LHG-8 and LG-770 melted under oxidizing conditions (1 atm O_2) is reported to be concentration dependent at impurity concentrations <300 ppmw Fe [90].

Scatter losses are due to inhomogeneities within the glass plus residual surface roughness after polishing. Scatter loss measurements have been reported [113] on polished pieces of LHG-8 and LG-750 meta-phosphate laser glasses (typical of the polished surfaces of glasses installed in an amplifier) using an integrating sphere scatterometer. The scatterometer is capable of measuring fractional losses to 10^{-5} of the incident intensity. Combined surface and interior scatter losses of less than 10^{-4} are reported [113].

6. Optical properties

6.1. Non-linear refractive index

A propagating laser beam can develop phase aberrations induced by changes in the glass refractive index at operating intensities greater than about 1 GW/cm^2. This effect degrades the beam focal spot, reduces the energy extraction efficiency of the laser and increases the risk of laser-induced damage [114–116].

The change in refractive index with laser intensity is given by [117,118]

$$n = n_0 + \gamma I, \tag{20}$$

where γ is the non-linear refractive index coefficient (m^2/W) and I is the laser intensity (W/m^2). Most commercial phosphate laser glasses have a non-linear index coefficient $\lesssim 3.5 \times 10^{-20}$ m^2/W. The intensity-dependent index causes amplitude ripples (noise), that occur at certain spatial

frequencies, to grow as exp(B) [116,119]. Here 'B' is the cumulative non-linear phase retardation integrated over the optical path length (z)

$$B = \frac{2\pi}{\lambda} \int \gamma I \, \mathrm{d}z. \tag{21}$$

Past experience has shown that for B greater than about 2 radians, unacceptable noise ripple growth can cause optical damage and also degrade the beam focus on large aperture laser systems [114,115].

Direct measurement of γ is difficult, so empirical correlations have been developed. The expression developed by Boling et al. [120] a number of years ago predicts γ from the refractive index (n_d) and the Abbe number (v) of the glass

$$\gamma = K(n_d - 1)(n_d^2 + 2)^2/\{n_d v[1.52 + (n_d^2 + 2) \times (n_d + 1)v/6n_d]^{1/2}\}, \tag{22}$$

where $K = 2.8 \times 10^{-10}$ m^2/W is an empirically determined constant. The non-linear refractive index, n_2 (in esu) is related to γ by $n_2 = \gamma(nc/40\pi)$, where c is light speed.

Fig. 10 shows the effect of a systematic change in modifiers from Be to Ba on n_2 for the meta-phosphate glass series $55P_2O_5$–$40RO$–$4.7La_2O_3$–$0.3Nd_2O_3$ as reported by Gan [28]. The data are correlated with the radius of the cation modifier. Also shown, for comparison, are the n_2s reported by Hayden et al. [39]. The results show the same trend as the work by Gan in that n_2 decreases, going from Ba to Mg. Based on these results, phosphate laser glasses with the smallest n_2 are those in which K and Mg are used as modifiers (assuming that the toxicity of Be makes it impractical). The laser glass, LG-770, has the smallest reported n_2 (and n_d) of any commercial phosphate laser glass; as discussed in Section 2, the modifiers used in LG-770 are Mg and K [7].

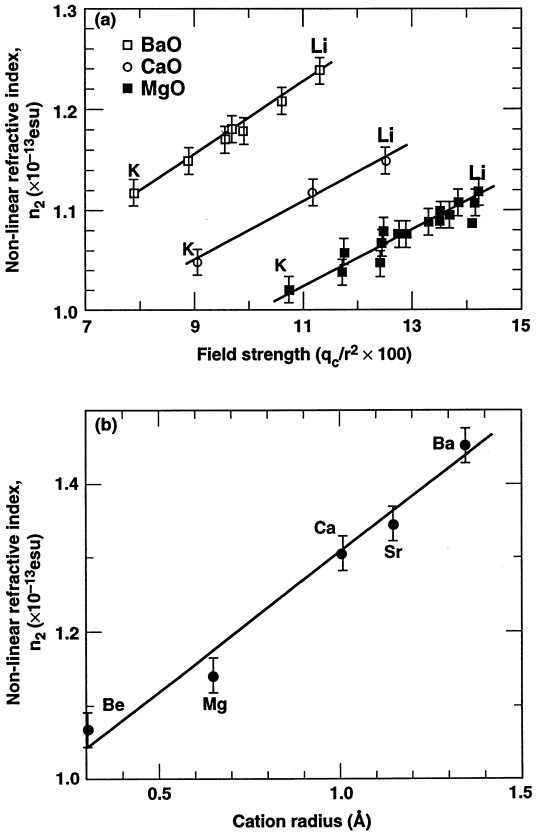

Fig. 10. Effect of systematic changes in combinations of group I and II modifiers on the non-linear index of phosphate laser glasses based on data from (a) Ref. [39] and (b) Ref. [28].

6.2. Thermal–optical properties

Laser glass must have optical homogeneity (Δn) of $< \pm 2 \times 10^{-6}$ to achieve the beam quality necessary to propagate and focus the output laser beam [7]. Thermal variations in the laser glass, caused by residual heat from the optical pumping process, can produce optical distortion by changing the optical path length. Therefore it is desirable to have a glass for which the temperature coefficient of the optical path length is zero (athermal glass). The change in the optical path length, ΔO_L (m), resulting from a temperature variation, ΔT (K), is given by [121]

$$\Delta O_L = \delta L \Delta T. \tag{23}$$

where L is the total path length (m) and δ is the temperature coefficient of the optical path length

$$\delta = \mathrm{d}n/\mathrm{d}T + (n - 1)\alpha_e. \tag{24}$$

The temperature change in refractive index ($\mathrm{d}n/\mathrm{d}T$) is defined by

$$dn/dT = [(n^2 - 1)(n^2 + 2)/6n](\phi - \beta), \quad (25)$$

where ϕ is the temperature-dependent coefficient of electronic polarizability (K^{-1}) and β is the volumetric thermal expansion coefficient (K^{-1}). For an isotropic material, such as glass, $\beta = 3\alpha_e$, where α_e is the linear coefficient of thermal expansion. An ideal athermal glass has $\delta = 0$ implying, from Eq. (24) that $dn/dT = (n-1)\alpha_e$, where n is usually ~1.5. Therefore, as a rule-of-thumb, a good athermal laser glass must have a dn/dT about half the coefficient of linear thermal expansion.

Toratani [32] and Izumitani and Toratani [122] report a method for calculating dn/dT for phosphate and silicate laser glasses, respectively, based on an additivity relationship for estimating the temperature coefficient of the electronic polarizability, ϕ:

$$\phi = \sum \phi_i X_i, \quad (26)$$

where ϕ_i is the additive contribution from glass component i and X_i is the component mole fraction. Table 2 lists ϕ_is for various common oxides in silicate [122] and phosphate [32] laser glasses. These data have been used to estimate dn/dT for a number of laser glasses [94] and in general, are in good agreement with measured data (see Table 2).

7. Thermal–mechanical properties

The figure-of-merit parameter commonly used to characterize the thermal–mechanical performance of laser glass is the well-known thermal shock resistance, R_s [93]:

$$R_s = k(1 - \mu)K_{IC}/(E\alpha_e), \quad (27)$$

where E is Young's modulus, k the thermal conductivity, K_{IC} the fracture toughness, μ Poisson's ratio and α_e is the coefficient of linear thermal expansion. R_s has units of $W/m^{1/2}$ and the larger R_s the greater the thermal loading without failure. Laser glasses can be subjected to thermal loads during handling and processing [123] as well as during operation [7,124].

There have been relatively few reported systematic studies of composition effects on thermal–mechanical properties of phosphate laser glasses. Hayden et al. [39] report the affects of varying alkali and alkaline earth modifiers in a meta-phosphate laser glass in which the Al_2O_3 and P_2O_5 contents are held constant. In an extension of this work, Elder et al. [123] systematically varied the network former; particularly the Al_2O_3/P_2O_5 ratio and the O/P ratio and also examined the effects of replacing P_2O_5 and Al_2O_3 with either SiO_2 or B_2O_3. In a study of glasses for repetition-rate lasers, Marion [124] analyzed data from Stokowski [20] in terms of a figure-of-merit similar to that

Table 2
Additivity factors, ϕ_i (10^{-6}/K), for estimating the temperature coefficient of electronic polarizability from the glass composition [32,122] and comparison of predicted vs. measured dn/dT reported for several phosphate laser glasses using these values [94]

	ϕ_i (10^{-6}/K)		dn/dT (10^{-6}/K)		
Component	Silicates	Phosphates	Glass	Predicted	Measured
SiO_2	17.4	20 (est.)	LHG-8	−4.8	−5.3
$PO_{0.5}$	–	20	LHG-80	−3.6	−3.8
$BO_{1.5}$	13.8	16	LG-750	−6.0	−6.8
$AlO_{1.5}$	22.2	26	LG-760	−4.9	−5.1
$LiO_{0.5}$	–	36 (est.)	HAP-3	1.0	1.9
$NaO_{0.5}$	50.0	44	APG-1	1.3	1.2
$KO_{0.5}$	43.9	45			
MgO	–	45 (est.)			
CaO	42.0	42 (est.)			
BaO	36.1	35			
PbO	50.2	47			
TiO_2	19.3	15			
ZnO	39.4	–			

given in Eq. (27). Jiang et al. [96] investigated the effects of groups I and II modifiers (K, Na, Li, Ba, Sr and Ca) on the thermal expansion coefficients of different phosphate laser glasses and report a correlation with cation electric field strength. Their data also show that glasses containing larger field strength cations (e.g., Li) have smaller thermal expansion coefficients. The above studies [39,96,123] all show that using modifiers with greater field strengths (particularly Li) increases Young's modulus and thermal conductivity and decreases the thermal expansion (e.g., see Fig. 11).

Improvements in thermal–mechanical properties tend to follow composition trends opposite to that for improved laser properties (see Sections 3 and 4). In general, optimizing the laser properties takes precedence over improving the mechanical properties so low field strength cations (e.g., K) are usually the dominant modifiers in a glass. The one exception is laser glass used in repetitively pulsed lasers (so-called HAP lasers). Here the need for good thermal shock resistance is critical therefore these glasses tend to contain larger field strength ions such as Li [32,33].

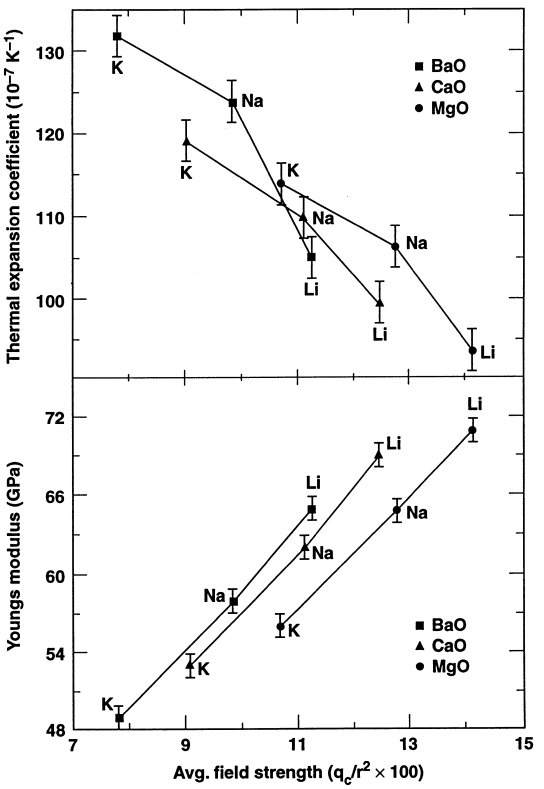

Fig. 11. Variation of linear thermal expansion coefficient and Young's modulus with the compositionally averaged field strength for phosphate laser glasses containing combinations of groups I and II modifiers (Li, Na, K, Mg, Ca and Ba). Plot generated from data by Hayden et al. [39]; the lines connect the data points and are added to distinguished data sets.

8. Fracture toughness and sub-critical crack growth

The size of the laser glass plates used in multi-kilojoule energy applications increases the threat of fracture due to increased thermal or mechanical-induced stress during handling and processing [7]. In addition, it is our experience that surface flaws ($\leqslant 1$ mm) may develop during operation due to laser or flashlamp-induced damage.

The fracture strength of phosphate laser glasses is less than that for silicate counterparts as indicated by fracture toughness measurements given in Table 3. In general, the fracture toughness for phosphate laser glasses is about one-half to two-thirds those for silicates.

Table 3
Fracture toughness values reported for common commercial phosphate and silicate laser glasses [94,125]

Glass (by vendor code name)	Vendor	Fracture toughness[b] (MPa $m^{1/2}$)
Phosphates		
LHG-8	Hoya	0.51 ± 0.02[a]
LG-770	Schott	0.43[a]
LG-750	Schott	0.45[c]
APG-1	Schott	0.61[a]
APG-2	Schott	0.64 ± 0.03[a]
IOG-1	Schott	0.54[a]
LHG-80	Hoya	0.46[a]
LHG-5	Hoya	0.42[c]
Silicates		
LG-680	Schott	0.86[a]
IOG-10	Schott	0.71[a]
LG-670[d]	Schott	0.83[c]
LSG91H	Hoya	0.88[c]

[a] Measured by the authors using chevron notch method [126].
[b] Error is ± 0.01 unless otherwise noted.
[c] Data from [125]; measured by indentation technique.
[d] Formerly ED-2 by Owens–Illinois.

Elder et al. [47] reported that fracture toughness varies with O/P ratio for a series of phosphate glasses containing Al, K and Ba. Their results show that the ultra-phosphates (O/P < 3) have greater fracture toughness.

Slow crack growth measurements have been reported recently by Crichton et al. [127] and Suratwala et al. [128] on the commercial phosphate glasses, LG-770 and LHG-8, respectively. Both studies have been carried out as a function of temperature (23–300°C) and water vapor pressure (0.3–355 mm Hg). In addition, Suratwala et al. [128] examined the effect of residual hydroxyl content in the laser glass. The results are analyzed using Wiederhorn's reaction rate model [129] for slow crack growth in region I (reaction kinetic limited region) and region II (mass transport limited region). Model parameters are reported for these two glasses that can be used to predict slow crack growth at different stress levels [127,128]. Both studies report regions of crack tip blunting where the crack growth rates depart from predictions made using the reaction rate model.

9. Laser-induced damage

The mega-joule lasers now under construction for inertial confinement fusion (ICF) research will produce peak fluences in the laser glass approaching 18–20 J/cm^2 with a peak irradiance of about 5.0 GW/cm^2 [130,131]. To avoid laser-induced optical damage the laser glass must be free of defects, specifically microscopic inclusions (either metallic or ceramic) left from the melting process. The most common inclusion source is metallic Pt inclusions from the Pt liners used in the melting system [7,132]. Prior to about 1990, Pt inclusion damage represented the major source of damage in laser glass used for high-peak-power applications [132,133]. However new processing methods effectively reduce the Pt inclusion concentration in phosphate laser glasses by more that 1000-fold to less than 0.1/litre [134–136]. For example, 50% of the large laser slabs ($79 \times 45 \times 4$ cm^3; 14 litre of glass each) used on the Beamlet laser at LLNL [130] are reported to have had no inclusions at all and the average for all the slabs produced is <0.1/litre [31]. Similar results have been reported for the several hundred replacement glass disks manufactured for the Nova and Phebus lasers [132,137]; each of those disks contained 7 litre of glass.

Inclusions in the laser glass damage at about between 2 and 5 J/cm^2 at the 1–10 pulse lengths typical of most HPP applications [132,138]. Although very small to begin with, inclusion damage can grow with successive laser shots to several millimeters or even centimeters in size eventually making the laser glass unusable [138]. Also large damage spots (>300 μm) in the laser glass can seed damage in other optics in the laser chain [114].

The new processing techniques used for eliminating Pt inclusions in phosphate glasses [132,134,135] rely on the intrinsic property of many phosphate glasses to dissolve Pt metal under oxidizing conditions. The effects of glass composition on platinum solubility have been reported to follow the trend: phosphate > silico–phosphate ≫ fluorophosphate > silicate [139]. In a similar study Hayden et al. [140] have examined the effects of the Al_2O_3 concentration in phosphate glasses on Pt solubility. They chose three commercial phosphate laser glasses (LG-770, LG-760 and APG-1) each having different Al_2O_3 content. These researchers report that the larger the Al_2O_3 content the smaller the Pt solubility. The effects of Al_2O_3 content on Pt solubility tend to parallel those reported by Izumitani et al. for SiO_2 content in phosphate glasses [139].

If inclusions inside the glass are eliminated then the damage threshold is limited only by the surface finish. The pulse length dependence of the surface damage threshold for polished glass samples (Fig. 12) can be represented by the empirical expression [131]

$$D_S\ (\mathrm{J/cm^2}) = 22 t_P^{0.4}, \tag{28}$$

where t_P is the laser pulse length (ns). The surface damage threshold approximately follows the $t^{1/2}$ relationship predicted by a thermal diffusion heat transport model [66,132]. For comparison, the damage threshold reported by Gonzales and

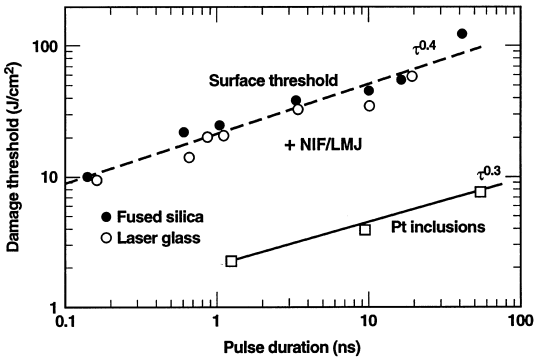

Fig. 12. Measured damage threshold at 1053 nm for Pt inclusions in laser glass as a function of laser pulse length; data are from [138]. Also shown, for comparison, are the measured damage thresholds at 1053 nm for highly polished laser glass and fused silica surfaces [131] and the design peak operating fluence of the NIF and LMJ mega-joule lasers currently under construction [1,130].

Milam [138] for Pt inclusions (Fig. 12) follows the approximate pulse length scaling relationship

$$D_{\mathrm{Pt}}\ (\mathrm{J/cm^2}) = 2t_{\mathrm{P}}^{0.3}. \tag{29}$$

Thus the presence of Pt inclusions reduces the operating limit of a laser glass by about 10-fold.

Jiang et al. [141] have investigated the redox equilibrium $[Pt^{4+} \leftrightarrows Pt^{2+} \leftrightarrows Pt^{0}]$ in a R_2O–BaO–P_2O_5 glass as a function of oxidizing environment and temperature. They assign absorption bands near 290, 360 nm and 320, 390 nm to Pt^{2+} and Pt^{4+}, respectively. By monitoring the relative peak amplitudes for these bands they report the ratio of Pt^{4+}/Pt^{2+} as a function of increasing oxygen partial pressure; $[Pt^{4+}/Pt^{2+}]\beta = P_{O_2}$ where β is about 0.75. They relate this same ratio to the observed Pt-inclusion density.

The tail of the ionic Pt absorption bands in the near UV extends into the visible, giving detectable absorption up to about 400 nm. This absorption can affect the energy storage of the laser glass because the absorption blocks some of the flashlamp radiation and reduces the pumping efficiency. The 400 nm absorption coefficient due to ionic Pt is generally specified not to exceed 0.25 cm^{-1} [31]; this coefficient corresponds to a Pt ion concentration of less than about 150 ppm [132]. For rods or slabs doped with $Nd^{3+} > 1 \times 10^{20}$ cm^{-3} the effect of the ionic Pt absorption is negligible as long as the absorption at 400 nm does not exceed about 0.25 cm^{-1}. Kelly et al. [142], however, have analyzed the effect of ionic Pt absorption on the flashlamp pumping of rods with smaller Nd-dopings. They estimate that an ionic Pt absorption at or near 0.25 cm^{-1} can reduce the pumping efficiency by up to 15% for 9.9 cm diameter laser glass rods doped with about 5×10^{19} Nd ions/cm^3.

10. Summary and directions for future work

We conclude this review with a summary (Table 4) of the properties and compositions of the Nd-doped phosphate laser glasses in use on major multi-kilojoule lasers in the US, Europe and Japan [8,94]. Glasses having optimal laser performance and acceptable thermal–physical properties are meta-phosphates having the approximate base composition: $60P_2O_5$–$10Al_2O_3$–$30K_2O$/MO, where MO is either BaO or MgO. Nd_2O_3 is generally added at doping levels of <2 mol% (i.e., $\lesssim 5 \times 10^{20}$ Nd^{3+}/cm^3). Small variations in composition and modifiers about this base glass composition have only minor effects (±10%) on most glass properties (see Table 4).

Non-radiative energy losses from the $^4F_{3/2}$ upper laser level are reasonably well understood. The one exception is OH quenching. Although an empirical relationship can be used to accurately estimate (±10%) the quenching effect, a theoretical formulation describing the unusual OH quenching affects at smaller Nd-doping is lacking and is worthy of further study. In addition, the mechanism and kinetics of dehydroxylation of phosphate glasses have received little attention despite the adverse effects of ppm levels of OH on many glass properties.

The development of processing technology for making inclusion-free phosphate glass has enabled lasers to be built and operated at fluences 5–10 times greater than was possible 10 years ago. However a detailed understanding of the mechanism of Pt dissolution in glasses bubbled with O_2

Table 4
Properties and compositions (when reported) of Nd-doped phosphate laser glasses in common use on high-energy/high-peak-power lasers [8]

Sources		Glass manufacturer				
		Hoya		Schott		Kigre
		[23,143]	[7,23,143]	[7]	[23,144]	[23,145]
Glass designation[a]	Symbol	LHG-80	LHG-8	LG-770	LG-750	Q88
Optical						
Refractive index						
@ 587.3 nm (±0.00002)[b]	n_d	1.5429	1.5296	1.5067	1.5257	1.5449
@ 1053 nm (±0.00015)[b]	n_1	1.5329	1.5201	1.4991	1.5160	1.5363
Non-linear refractive index						
(10^{-13} esu)	n_2	1.24	1.12	1.01	1.08	1.14
(10^{-20} m^2/W)	γ	3.36	3.08	2.78	2.98	3.11
Abbe number (±0.05)	v	64.7	66.5	68.4	68.2	64.8
Temp-coeff. refract. index (10^{-6}/K) (±0.5)	dn/dT	−3.8	−5.3	−4.7	−5.1	−0.5
Temp-coeff. optical path (10^{-6}/K) (±0.2)	δ	1.8	0.6	1.2	0.8	2.7
Laser						
Emission cross-section (10^{-20} cm^2) (±0.2)	σ_{em}	4.2	3.6	3.9	3.7	4.0
Saturation fluence (J/cm^2) (calc.)	F_{sat}	4.5	5.2	4.8	5.1	4.7
Radiative lifetime (zero-Nd) (μs) (±3)	τ_o	337	365	372	383	326
Judd–Ofelt radiative lifetime (μs) (±10%)	τ_r	327	351	349	367	326
Judd–Ofelt parameters (10^{-20} cm^2) (±5%)	Ω_2	3.6	4.4	4.3	4.6	3.3
	Ω_4	5.0	5.1	5.0	4.8	5.1
	Ω_6	5.5	5.6	5.6	5.6	5.6
Emission band width (nm) (±0.1)	$\Delta\lambda_{eff}$	23.9	26.5	25.4	25.3	21.9
Conc. quenching factor[c] (×10^{20} cm^{-3}) (±0.3)	Q	10.1	8.4	8.8	7.4	6.6
Fluorescence peak (nm) (±0.3)	λ_L	1054	1053	1053	1053.5	1054
Thermal						
Thermal conduct. (W/m K) (±0.03)	k	0.59	0.58	0.57	0.60	0.84
Thermal diffusivity (10^{-7} m^2/s)	α	3.2	2.7	2.9	2.9	–
Specific heat (J/g K) (±0.02)	C_p	0.63	0.75	0.77	0.72	0.81
Coeff. thermal expan.[d] (10^{-7}/K) (±3)	α_e	130	127	134	132	104
Glass transition temp (°C) (±5)	T_g	402	485	461	450	367
Mechanical						
Density (g/cm^3) (±0.01)	ρ	2.92	2.83	2.59	2.83	2.71
Poisson's ratio (±0.01)	μ	0.27	0.26	0.25	0.26	0.24
Fracture toughness (Mpa m$^{0.5}$) (±0.02)	K_{IC}	0.46	0.51	0.43	0.45	–
Hardness (GPa) (±0.10)	H	3.35	3.43	3.58	2.85	–
Young's modulus (GPa) (±1.0)	E	50	50	47	50	70

[a] LHG-8: (56–60)P_2O_5–(8–12)Al_2O_3–(13–17)K_2O–(10–15)BaO–(0–2)Nd_2O_3; LG-770: (58–62)P_2O_5–(6–10)Al_2O_3–(20–25)K_2O–(5–10)MgO–(0–2)Nd_2O_3; LG-750: (55-60)P_2O_5–(8–12)Al_2O_3–(13–17)K_2O–(10–15)BaO–(0–2)Nd_2O_3.
[b] Values vary slightly with Nd-doping levels.
[c] Q defined by Eq. (14).
[d] 20–300°C.

or Cl_2 is lacking. In addition, the effects of glass composition and structure on the dissolution process are poorly understood. For example, the reasons why SiO_2 and Al_2O_3 additions to metaphosphate glasses retard Pt inclusion dissolution is not well understood.

Finally, glass compositions have been developed with good laser performance properties but a corresponding quantitative understanding (i.e., able to be reduced to calculation) of the relationship between glass structure and performance is lacking and remains a continuing challenge.

Acknowledgements

The authors gratefully acknowledge the many helpful discussions with co-workers, Dr J. Hayden and Dr A. Marker at Schott Glass Technologies, Inc. and Dr H. Toratani and Mr K. Takeuchi at Hoya Corporation. The assistance by Ms G. Martinez in the literature search for this review and by Ms A. Clasen in the preparation of the manuscript is also deeply appreciated. Work was performed under the auspices of the US Department of Energy by Lawrence Livermore National Laboratory under Contract No. W-7405-Eng-48.

References

[1] J.R. Murray, A walk through the National Ignition Facility, ICF Quarterly Report, Lawrence Livermore National Laboratory Report UCRL-LR-105821-97, 7, 1997, p. 95.
[2] M. Andre, M. Novaro, D. Schirmann, Chocs. Rev. Sci. Techn. Direct. Appli. Milit. 13 (1995) 73.
[3] S. Nakai, Optoelectron. Devices Technol. 8 (1993) 147.
[4] G. Theill, H. Graillot, P. Joly, A. Boscheron, L. Videau, A. Adolf, Fusion Eng. Des. 44 (1999) 157.
[5] T.R. Boehly, D.L. Brown, R.S. Craxton, R.L. Keck, J.P. Knauer, J.H. Kelly, T.J. Kessler, S.A. Kumpan, S.J. Loucks, S.A. Letzring, F.J. Marshall, R.L. McCrory, S.F.B. Morse, W. Seka, J.M. Soures, C.P. Verdon, Opt. Commun. 133 (1997) 495.
[6] J. Lindl, Phys. Plasmas 2 (1995) 3933.
[7] J. Campbell, T. Suratwala, C. Thorsness, J. Hayden, A. Thorne, A. Marker, K. Takeuchi, M. Smolley, G. Ficini-Dorn, these Proceedings, p. 342.
[8] J.H. Campbell, 25 years of laser glass development leading to a 1.8 MJ, 500 TW laser for fusion ignition, Lawrence Livermore National Laboratory Report, UCRL-JC-129507, 1998, p. 1.
[9] H. Ebendorff-Heidepriem, D. Ehrt, M. Bettinelli, A. Speghini, J. Non-Cryst. Solids 240 (1998) 66.
[10] H. Ebendorff-Heidepriem, D. Ehrt, Glastech. Ber. Glass Sci. Technol. 71 (1998) 289.
[11] H. Ebendorff-Heidepriem, W. Seeber, D. Ehrt, Glastech. Ber. Glass Sci. Technol. 66 (1993) 235.
[12] S. Jiang, M. Myers, N. Peyghambarian, J. Non-Cryst. Solids 239 (1998) 143.
[13] S. Jiang, T. Luo, B.C. Hwang, G. Nunzi-Conti, M. Myers, D. Rhonehouse, S. Honkanen, N. Peyghambarian, Opt. Eng. 37 (1998) 3282.
[14] G.K.D. Mohapatra, Phys. Chem. Glasses 40 (1999) 57.
[15] S.T. Davey, B.J. Ainslie, R. Wyatt, in: M.J. Weber (Ed.), CRC Handbook of Laser Science and Technology, CRC, Boca Raton, FL, 1995, p. 635.
[16] M.J. Weber, J. Non-Cryst. Solids 123 (1990) 208.
[17] K. Church, R. Zanoni, D. Sapak, J. Hayden, SPIE 2287 (1994) 97.
[18] P.R. Morkel, K.P. Jedrzejewski, E.R. Taylor, IEEE J. Quantum Electron. 29 (1993) 2178.
[19] N. Neuroth, Opt. Eng. 26 (1987) 96.
[20] S.E. Stokowski, Laser glass: an engineered material, Lawrence Livermore National Laboratory Report UCRL-96331, 1987, p. 1.
[21] R. Reisfeld, M. Eyal, C.K. Jorgensen, J. Less Common Met. 126 (1986) 187.
[22] M.J. Weber, Laser glasses, Lawrence Livermore National Laboratory Report UCRL-UC-109922, 1992.
[23] S.E. Stokowski, R.A. Saroyan, M.J. Weber, Laser glass Nd-doped glass spectroscopic and physical properties, Lawrence Livermore National Laboratory Report M-095, Rev. 2, vols. 1&2, 1981.
[24] N.E. Alekseev, V.P. Gapontsev, M.E. Zhabotinskii, V.B. Kravchenko, Y.P. Rudnitskii, Laser Phosphate Glasses, Nauka, Moscow, 1980 (English Translation, Lawrence Livermore National Laboratory Report UCRL-Trans-11817, 1983).
[25] S.E. Stokowski, in: M.J. Weber (Ed.), Handbook of Laser Science and Technology, vol. 1, CRC, Boca Raton, FL, 1982, p. 1.
[26] J.E. Marion, M.J. Weber, Eur. J. Solid-State Inorg. Chem. 28 (1991) 271.
[27] C.F. Rapp, in: M.J. Weber (Ed.), CRC Handbook of Laser Science and Technology, CRC, Boca Raton, FL, 1995, p. 619 (Sect. 17.1).
[28] F. Gan, Chin. Phys. 5 (1985) 145.
[29] E.V. Uhlmann, M.C. Weinberg, N.J. Kreidl, L.L. Burgner, R. Zanoni, K.H. Church, J. Non-Cryst. Solids 178 (1994) 15.
[30] J.L. Emmett, W.F. Krupke, J.B. Trenholme, The future development of high-power solid state laser systems, Lawrence Livermore National Laboratory Report UCRL-53344, 1982.
[31] J.H. Campbell, L.J. Atherton, J.J. DeYoreo, M.R. Kozlowski, R.T. Maney, R.C. Montesanti, L.M. Sheehan, C.E. Barker, Large-aperture, high-damage-threshold optics for beamlet, ICF Quarterly Report, Lawrence Livermore National Laboratory Report UCRL-LR-105821-95-1, 1994, p. 52.

[32] H. Toratani, PhD thesis, Kyoto University, Kyoto, Japan, 1989.
[33] T. Izumitani, M. Matsukawa, C. Hata, K. Tanaka, H. Toratani, Laser Induced Damage in Optical Materials, 1986, NIST Publication 752, 1988, p. 13.
[34] H. Takebe, Y. Nageno, K. Morinaga, J. Am. Ceram. Soc. 78 (1995) 1161.
[35] H. Takebe, K. Morinaga, T. Izumitani, J. Non-Cryst. Solids 178 (1994) 58.
[36] Y. Lu, N. Ming, J. Mater. Sci. 30 (1995) 5705.
[37] M. Sen, M. Hanfen, Chin. Phys. 6 (1986) 657.
[38] S. Jiang, Y. Jiang, Glastech. Ber. Glass Sci. Technol. 64 (1991) 291.
[39] J.S. Hayden, Y.T. Hayden, J.H. Campbell, SPIE 1277 (1990) 121.
[40] J.O. Byun, B.H. Kim, K.S. Hong, H.J. Jung, S.W. Lee, K.S. Ryoo, A.A. Izyneev, V.B. Kravchenko, Jpn. J. Appl. Phys. 33 (1994) 4907.
[41] L.M. Cook, A.J. Marker, SPIE 505 (1984) 102.
[42] S.P. Tandon, Y.K. Sharma, N.B. Bishnoi, K. Tandon, Def. Sci. J. 47 (1997) 225.
[43] Z. Jiang, X. Song, J. Zhang, Studies of Laser Phosphate Glasses, Glass Division Meeting, Conference of the Chinese Silicates Society, October 1980 (English translation, Lawrence Livermore National Laboratory Report UCIR-1683, 1987, p. 1).
[44] A.R. Kuznetsov, S.G. Lunter, S.I. Nikitina, A.G. Plyukhin, Y.K. Fedrov, J. Appl. Spectrosc. 56 (1992) 68.
[45] H. Ebendorff-Heidepreim, W. Seeber, D. Ehrt, J. Non-Cryst. Solids 183 (1995) 191.
[46] A.Z. Dietzel, Z. Electrochem. 48 (1942) 9.
[47] S. Payne, M.L. Elder, J.H. Campbell, G.D. Wilke, M.J. Weber, in: A.J. Bruce, B.V. Hiremath (Eds.), Solid-State Optical Materials, vol. 28, American Ceramic Society, Westerville, OH, 1991, p. 253.
[48] R. Brow, R. Kirkpatrick, G. Turner, J. Am. Ceram. Soc. 73 (1990) 2293.
[49] R. Brow, J. Am. Ceram. Soc. 76 (1993) 913.
[50] R. Brow, R. Kirkpatrick, G. Turner, J. Am. Ceram. Soc. 76 (1993) 919.
[51] H.B. Senin, Q. Wang, G.A. Saunders, R.C. Draper, E.F. Lambson, M. Cankurtaran, F.J. Ford, H.M. Farok, H.A.A. Sidek, W.A. Lambson, Glass Technol. 34 (1993) 75.
[52] J.J. Hudgens, R.K. Brow, D.R. Tallant, S.W. Martin, J. Non-Cryst. Solids 223 (1998) 21.
[53] Y. Jin, X. Chen, X. Huang, J. Non-Cryst. Solids 112 (1989) 147.
[54] R.K. Brow, D.R. Tallant, Z.A. Osborne, Y. Yang, D.E. Day, Phys. Chem. Glasses 32 (1991) 188.
[55] R. Brow, C. Phifer, G. Turner, R. Kirkpatrick, J. Am. Ceram. Soc. 74 (1991) 1287.
[56] D. Day, J. Non-Cryst. Solids 112 (1989) 7.
[57] R.K. Brow, D.R. Tallant, J.J. Hudgens, S.W. Martin, A.D. Irwin, J. Non-Cryst. Solids 177 (1994) 221.
[58] R.K. Sato, R.J. Kirkpatrick, R.K. Brow, J. Non-Cryst. Solids 143 (1992) 257.
[59] R.K. Brow, D.R. Tallant, J. Non-Cryst. Solids 222 (1997) 396.
[60] R.J. Kirkpatrick, R.K. Brow, Solid-State Nucl. Magn. Reson. 5 (1995) 9.
[61] W. Seeber, D. Ehrt, Silikattechnik 41 (1990) 230.
[62] T. Izumitani, H. Toratani, H. Kuroda, J. Non-Cryst. Solids 47 (1982) 87.
[63] R.C. Powell, Physics of Solid-State Laser Materials, Springer, New York, 1998.
[64] M. Gerloch, Orbitals, Terms and States, Wiley, Chichester, 1986.
[65] S. Hufner, Optical Spectra of Transparent Rare Earth Compounds, Academic Press, New York, 1978.
[66] W. Koechner, Solid-State Laser Engineering, 4th Ed., Springer, New York, 1996.
[67] H.T. Powell, A.C. Erlandson, K.S. Jancaitis, J.E. Murray, SPIE 1277 (1990) 103.
[68] A.C. Erlandson, K.S. Jancaitis, R.W. McCracken, M.D. Rotter, Gain uniformity and amplified spontaneous emission in multi-segment amplifiers, ICF Quarterly Report, Lawrence Livermore National Laboratory Report UCRL-JC-111172, 1992, p. 105.
[69] R. Beach, Laser Tech. Briefs 2 (1994) 32.
[70] J.K. Crane, M. Martinez, R.J. Beach, S. Mitchell, F. Penko, D. Browning, R. Wilcox, Diode-pumped regenerative amplifier for the NIF laser system, ICF Quarterly Report, Lawrence Livermore National Laboratory Report UCRL-LR-105821-97-4, 1997, p. 246.
[71] C.B. Layne, W.H. Lowdermilk, M.J. Weber, Phys. Rev. B 16 (1977) 110.
[72] C. Bibeau, S. Payne, H. Powell, J. Opt. Soc. Am. B 12 (1995) 1981.
[73] C. Bibeau, S. Payne, Terminal-level relaxation in nd-doped laser materials, ICF Quarterly Report, Lawrence Livermore National Laboratory Report UCRL-LR-105821-95-2, 1995, p. 119.
[74] C. Bibeau, J. Trenhome, S. Payne, IEEE J. Quantum Electron. 32 (1996) 1487.
[75] S. Payne, C. Bibeau, J. Lumin. 79 (1998) 143.
[76] T. Förster, Ann. Phys. 2 (1948) 56.
[77] D.L. Dexter, J. Chem. Phys. 21 (1953) 836.
[78] W. Krupke, IEEE J. Quantum Electron. QE-10 (1974) 450.
[79] B.R. Judd, Phys. Rev. B 127 (1962) 750.
[80] G.S. Ofelt, J. Chem. Phys. 37 (1962) 511.
[81] S. Lunter, A. Dymnikov, A. Przhevuskii, Y. Federov, SPIE 1513 (1991) 349.
[82] Y. Nageno, H. Takebe, K. Morinaga, J. Am. Ceram. Soc. 76 (1993) 3081.
[83] H. Takebe, Y. Nageno, K. Morinaga, J. Am. Ceram. Soc. 77 (1994) 2132.
[84] H. Ebendorff-Heidepriem, D. Ehrt, M. Bettinelli, A. Speghini, SPIE 3622 (1999) 19.
[85] R.R. Jacobs, M.J. Weber, IEEE J. Quantum Electron. QE-12 (1976) 102.
[86] X.J. Xu, C.S. Ray, Solid-State Opt. Mater. 28 (1992) 297.
[87] J. Caird, A. Ramponi, P. Staver, J. Opt. Soc. Am. B 8 (1991) 1391.

[88] A.C. Erlandson, M.D. Rotter, D.N. Frank, R.W. McCracken, Design and performance of the beamlet amplifiers, ICF Quarterly Report, Lawrence Livermore National Laboratory Report UCRL-LR-105821-95-1, 1994, p. 18.
[89] S.E. Stokowski, D. Krashkevich, Mater. Res. Soc. Symp. 61 (1986) 273.
[90] P. Ehrmann, J.H. Campbell, T.I. Suratwala, J.S. Hayden, D. Krashkevich, K. Takeuchi, J. Non-Cryst. Solids, 1999, this conference.
[91] C.B. Layne, M.J. Weber, Phys. Rev. B 16 (1977) 3259.
[92] S.A. Payne, C.D. Marshall, A. Bayramian, G.D. Wilke, J.S. Hayden, Appl. Phys. B 61 (1995) 257.
[93] S.E. Stokowski, L. Cook, H. Mueller, M.J. Weber, J. Lumin. 31&32 (1984) 823.
[94] J.H. Campbell, SPIE CR 64 (1996) 3.
[95] A.I. Burshtein, Soviet Phys., JETP 35 (1972) 882.
[96] Y. Jiang, S. Jiang, Y. Jiang, J. Non-Cryst. Solids 112 (1989) 286.
[97] J.O. Byun, B.H. Kim, K.S. Hong, H.J. Jung, S.W. Lee, K.S. Ryoo, A.A. Izyneev, V.B. Kravchenko, Jpn. J. Appl. Phys. 33 (1994) 4907.
[98] S.A. Payne, G.D. Wilke, L.K. Smith, W.F. Krupke, Opt. Commun. 111 (1994) 263.
[99] D. Zhuo, W. Xu, Y. Jiang, Chin. Phys. 6 (1986) 157.
[100] J. Shelby, Handbook of Gas Diffusion in Solids and Melts, ASM International, Materials Park, OH, 1996, p. 217.
[101] H. Ebendorff-Heidepriem, D. Ehrt, Glastech. Ber. Glass Sci. Technol. 68 (1995) 139.
[102] H. Toratani, H.E. Meissner, T. Izumitani, S.E. Stokowski, J. Non-Cryst. Solids 95&96 (1987) 701.
[103] A. Matthai, D. Ehrt, C. Rüssel, Glastech. Ber. Glass Sci. Technol. 71 (1998) 187.
[104] D. Sapak, J. Ward, J. Marion, SPIE 970 (1988) 107.
[105] K. Zirkelbach, R. Bruckner, Glastech. Ber. Glass Sci. Technol. 60 (1987) 312.
[106] L.B. Glebov, E.N. Boulos, J. Non-Cryst. Solids 242 (1998) 49.
[107] C.R. Kurkjian, E.A. Sigety, Phys. Chem. Glasses 9 (1968) 73.
[108] D. Ehrt, W. Seeber, J. Non-Cryst. Solids 129 (1991) 19.
[109] D. Ehrt, M. Leister, A. Matthai, Molten Salt Forum 5&6 (1998) 547.
[110] B. Camara, Glastech. Ber. Glass Sci. Technol. 51 (1978) 87.
[111] U. Kolberg, in: H. Bach, N. Neuroth (Eds.), The Properties of Optical Glass, Springer, Berlin, 1995, p. 351 (Chapter 8.8).
[112] A.M. Bishay, L. Makar, J. Am. Ceram. Soc. 52 (1969) 605.
[113] J.A. Caird, F.P. Milanovich, N.D. Nielsen, H.T. Powell, J.E. Marion, A.J. Pertica, J.N. Roe, in: Conference on Lasers and Electro-Optics (CLEO), 1989, p. 1.
[114] J.T. Hunt, K.R. Manes, P.A. Renard, Appl. Opt. 32 (1993) 5973.
[115] J.T. Hunt, D.R. Speck, Opt. Eng. 28 (1989) 461.
[116] J. Hunt, J. Glaze, W. Simmons, P. Renard, Appl. Opt. 17 (1978) 2053.
[117] D.C. Brown, High-Peak-Power Nd: Glass Laser Systems, Springer, New York, 1981.
[118] B.E.A. Saleh, M.C. Teich, Fundamentals of Photonics, Wiley, New York, 1991.
[119] W. Simmons, J. Hunt, W. Warren, IEEE J. Quantum Electron. QE-17 (1981) 1727.
[120] N. Boling, A. Glass, A. Owyoung, IEEE J. Quantum Electron. QE-14 (1978) 601.
[121] D.R. Uhlmann, N.J. Kreidl, Optical Properties of Glass, American Ceramic Society, Westerville, OH, 1991.
[122] T. Izumitani, H. Toratani, J. Non-Cryst. Solids 49 (1980) 611.
[123] M.L. Elder, Y.T. Hayden, J.H. Campbell, S.A. Payne, G.D. Wilke, in: A.J. Bruce, B.V. Hiremath (Eds.), Solid-State Optical Materials, vol. 28, American Ceramic Society, Westerville, OH, 1991, p. 261.
[124] J.E. Marion, SPIE 1128 (1989) 318.
[125] W.F. Krupke, M.D. Shinn, J.E. Marion, J.A. Caird, S.E. Stokowski, J. Opt. Soc. Am. B 3 (1986) 102.
[126] K.P.R. Reddy, E.H. Fontana, J.D. Helfinstine, J. Am. Ceram. Soc. 71 (1988) C310.
[127] S. Crichton, M. Tomozawa, J. Hayden, T. Suratwala, J. Campbell, J. Am. Ceram. Soc. 82 (1999) 3097.
[128] T.I. Suratwala, R.A. Steele, G.D. Wilke, J.H. Campbell, K. Takeuchi, these Proceedings, p. 213.
[129] S. Wiederhorn, J. Am. Ceram. Soc. 50 (1967) 407.
[130] B.M. Van Wonterghem, J.R. Murray, J.H. Campbell, D.R. Speck, C.E. Barker, I.C. Smith, D.F. Browning, W.C. Behrendt, Appl. Opt. 36 (1997) 4932.
[131] J.H. Campbell, F. Rainer, M. Kozlowski, C.R. Wolfe, I.M. Thomas, F. Milanovich, SPIE 1441 (1990) 444.
[132] J.H. Campbell, E.P. Wallerstein, J.S. Hayden, D.L. Sapak, D.E. Warrington, A.J. Marker, H. Toratani, H. Meissner, S. Nakajima, T. Izumitani, Elimination of platinum inclusions in phosphate laser glasses, Lawrence Livermore National Laboratory Report UCRL-53932, 1989, p. 1.
[133] Fundamentals of Damage in Laser Glass, National Materials Advisory Board, Division of Engineering, National Research Council, NMAB-271, 1970.
[134] J.H. Campbell, E.P. Wallerstein, J.S. Hayden, D.L. Sapak, D.E. Warrington, A.J. Marker, Glastech. Ber. Glass Sci. Technol. 68 (1995) 11.
[135] J.H. Campbell, E.P. Wallerstein, H. Toratani, H.E. Meissner, S. Nakajima, T.S. Izumitani, Glastech. Ber. Glass Sci. Technol. 28 (1995) 59.
[136] J.H. Campbell, Glastech. Ber. Glass Sci. Technol. 68 (1995) 96.
[137] C.L. Weinzapfel, G.J. Greiner, C.D. Walmer, J.K. Kimmons, E.P. Wallerstein, F.T. Marchi, J.H. Campbell, J.S. Hayden, K. Komiya, T. Kitiyama, Laser Induced Damage in Optical Materials, National Institute of Standards and Technology Special Publication, 756, 1987, p. 112.
[138] R. Gonzales, D. Milam, Laser Induced Damage in Optical Materials, National Bureau of Standards Special Publication, 745, 1988, p. 128.

[139] T. Izumitani, M. Matsukawa, H. Miyade, Laser Induced Damage in Optical Materials, National Institute of Standards and Technology Special Publication, 756, 1988, p. 29.
[140] Y.T. Hayden, J.H. Campbell, S.A. Payne, G.D. Wilke, in: A.J. Bruce, B.V. Hiremath (Eds.), Solid-State Optical Materials, vol. 28, American Ceramic Society, Westerville, OH, 1992, p. 283.
[141] C. Jiang, D. Zhuo, J. Zhang, Chin. J. Lasers A 23 (1996) 1047.
[142] J.H. Kelly, M.H. Shoup, SPIE 1627 (1992) 175.
[143] Laser Glass Product Catalog, Hoya Corporation USA, Fremont, CA, 1994, p. 1.
[144] Laser Glass Product Catalog, Schott Glass Technologies, Duryea, PA, 1999, p. 1.
[145] Laser Glass Product Catalog, Kigre, Hilton Head, SC, 1990, p. 1.